nature neuroscience

SUPPLEMENTARY INFORMATION
https://doi.org/10.1038/s41593-018-0334-7

In the format provided by the authors and unedited.

Increased synapse elimination by microglia in schizophrenia patient-derived models of synaptic pruning

Carl M. Sellgren[1,2,3]*, Jessica Gracias[1,2,3], Bradley Watmuff[1,2], Jonathan D. Biag[4], Jessica M. Thanos[1,2], Paul B. Whittredge[4], Ting Fu[1,2], Kathleen Worringer[4], Hannah E. Brown[1,2], Jennifer Wang[1,2], Ajamete Kaykas[4], Rakesh Karmacharya[1,2,5], Carleton P. Goold[4], Steven D. Sheridan[1,2] and Roy H. Perlis[1,2]*

[1]Center for Quantitative Health, Center for Genomic Medicine and Department of Psychiatry, Massachusetts General Hospital, Boston, MA, USA. [2]Department of Psychiatry, Harvard Medical School, Boston, MA, USA. [3]Department of Physiology and Pharmacology, Karolinska Institutet, Stockholm, Sweden. [4]Novartis Institutes for BioMedical Research, Cambridge, MA, USA. [5]Schizophrenia and Bipolar Disorder Program, McLean Hospital, Belmont, MA, USA. *e-mail: carl.sellgren@ki.se; rperlis@mgh.harvard.edu

Supplementary Figure 1.

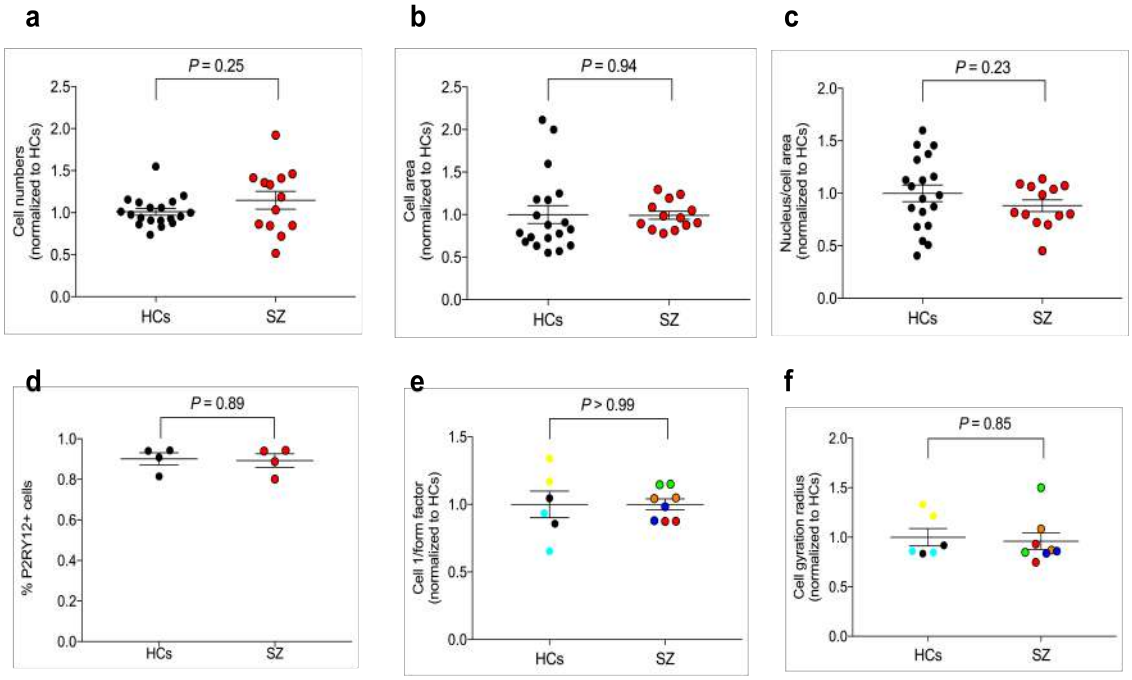

Supplementary Figure 1. Characteristics of induced microglia-like cells (iMGs). (**a**) – (**c**) display cell numbers, cell area (um), and nucleus / cell body area ratio for individuals included in comparison of phagocytic uptake of synaptosomes (Fig. 3c) between healthy controls (HCs; n = 19) and schizophrenia subjects (SZ; n = 13). Multiple transdifferentiations per subject are plotted as one mean. All data normalized to HCs. We also confirmed lack of influence of these parameters on phagocytic index (i.e. PSD-95 engulfment) (**a**)r = 0.09; P = 0.62, (**b**) r = -0.1; P = 0.58, and (**c**) r = 0.008; P = 0.96, respectively. Each comparison is based on data from 38,967 cells. (**d**) Transdifferentiation yielded around 90% purity as assessed by positive staining for the microglial-enriched protein P2RY12 across a subset of 4 HCs and 4 SZ subjects. Based on a total of and based on data from 4,467 cells. (**e**) and (**f**) display measurements of cell shape homogeneity for a subset of 3 HCs vs. 4 SZ subjects with 2 transdifferentiations per subject plotted individually and in same color. All data normalized to HCs. Groups were compared using *t*-tests in panel a – c and in d – f using a Mann-Whitney *U*-test. All reported p-values are two-sided. Mean and SEM is shown in each plot.

Supplementary Figure 2.

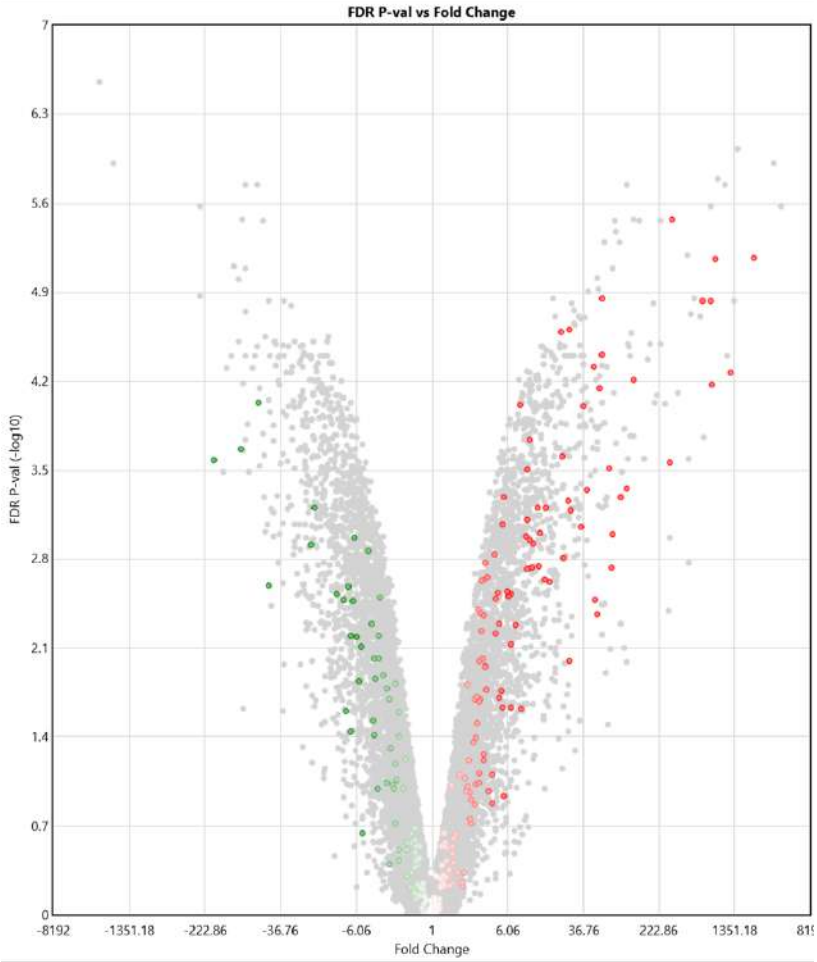

Supplementary Figure 2. Log 2 fold changes (mRNA expression in monocytes, n = 2 subjects, vs. induced microglia-like cells [iMGs], n = 3 subjects) plotted against FDR-adjusted (Benjamini-Hochberg) two-sided p-values (derived from one-way ANOVAs). Red (higher expression in iMGs) and green (higher expression in monocytes) indicate microglia-specific genes as reported by Bennett, M.L.*, et al.* (New tools for studying microglia in the mouse and human CNS. *Proc Natl Acad Sci U S A* **113**, E1738-1746 (2016)).

Supplementary Figure 3

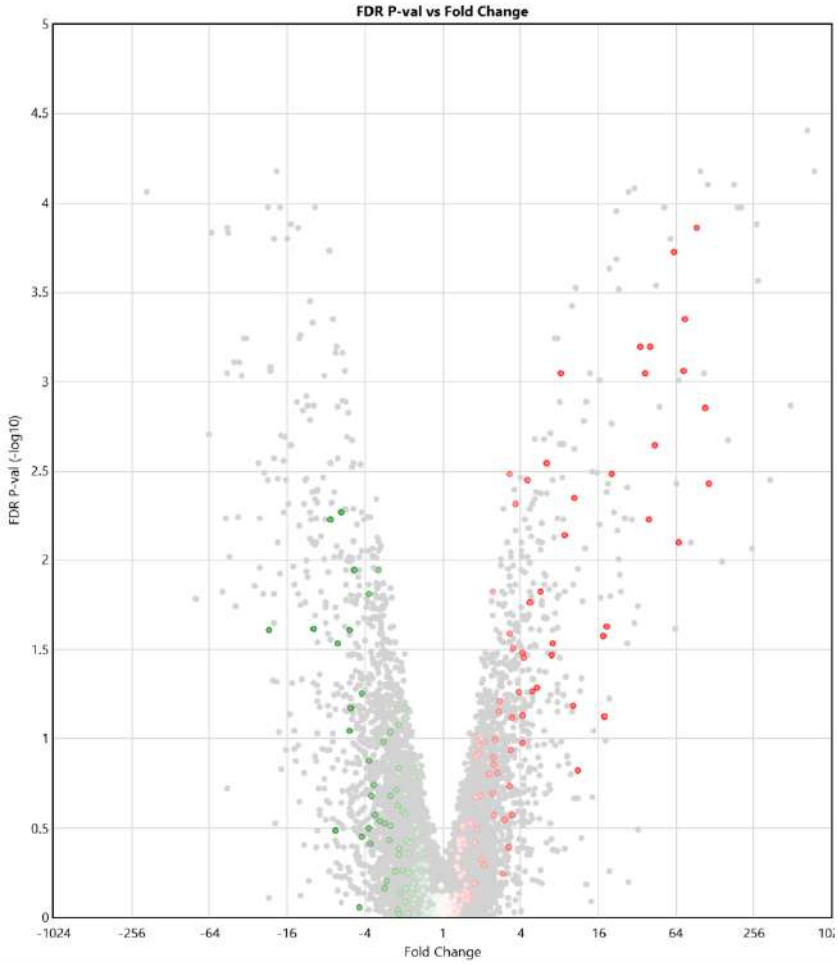

Supplementary Figure 3. Log 2 fold changes (mRNA expression in monocytes-derived macrophages, n=3, vs. induced microglia-like cells [iMGs], n=3) plotted against FDR-adjusted (Benjamini-Hochberg) two-sided p-values (derived from one-way ANOVAs). Red (higher expression in iMGs) and green (higher expression in monocytes) indicate microglia-specific genes as reported by Bennett, M.L.*, et al.* (New tools for studying microglia in the mouse and human CNS. *Proc Natl Acad Sci U S A* **113**, E1738-1746 (2016)).

Supplementary Figure 4

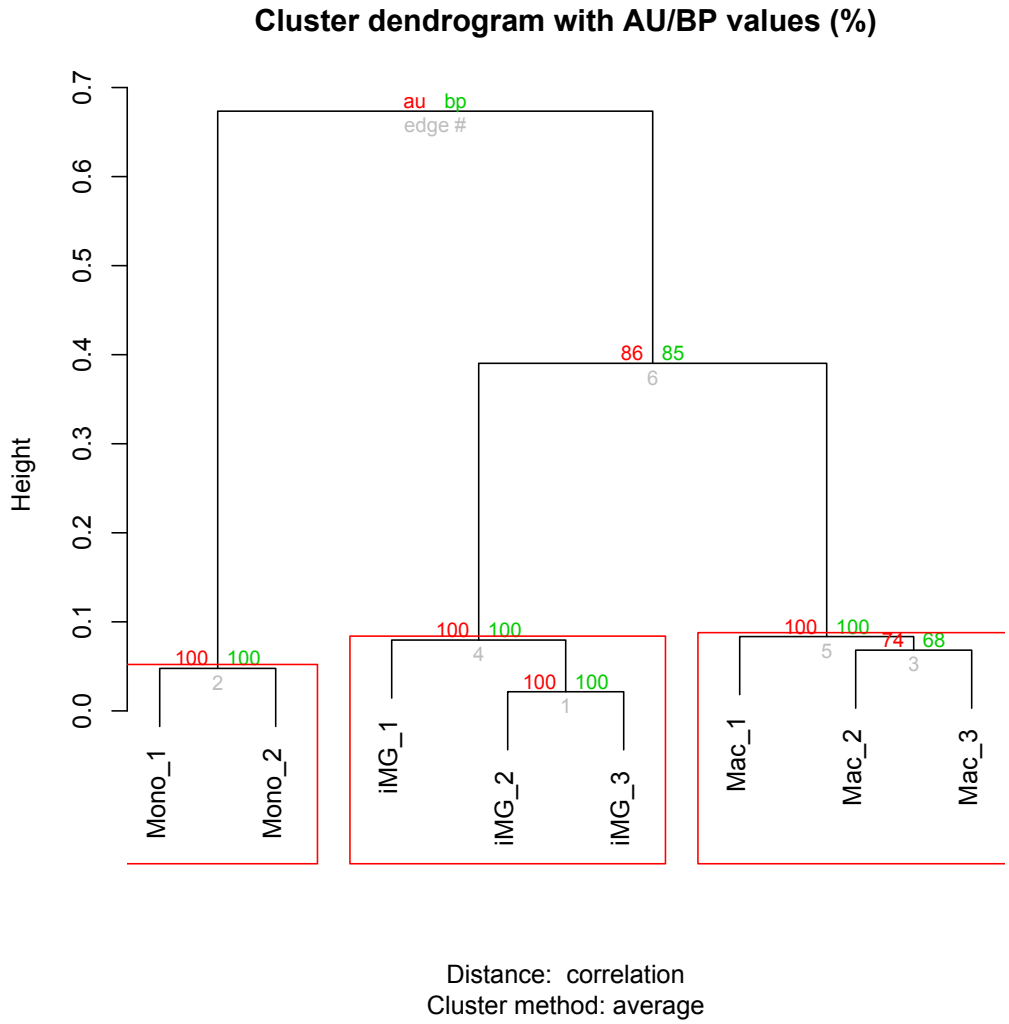

Supplementary Figure 4. Hierarchical cluster analysis (correlation as distance metric) of mRNA expression in monocytes (Mono), monocyte-derived macrophages (Mac), and induced microglia-like cells (iMGs), using the R package pvclust. Uncertainty in clustering is assessed via multiscale bootstrap resampling (nboot = 10,000) and Approximately Unbiased (AU) probability value as well as ordinary Bootstrap Probability (BP) value is provided for each cluster. Clusters with a significance level below 0.05, corresponds to AU/BP>95, are highlighted.

Supplementary Figure 5

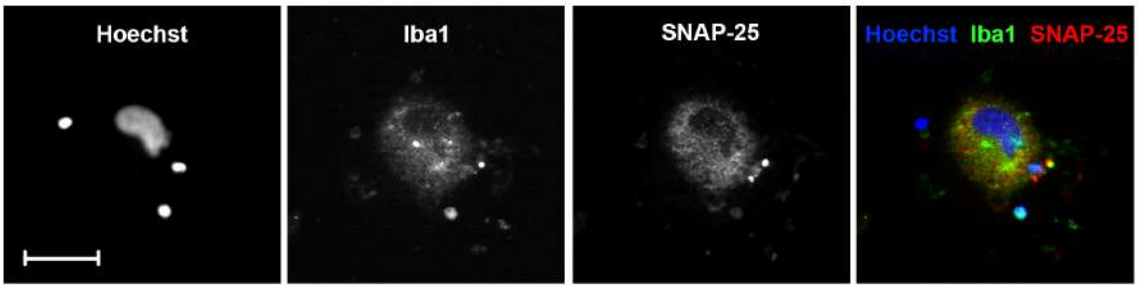

Supplementary Figure 5. Co-localization and engulfment of the pre-synaptic marker SNAP25 (red) by iMGs (green, IBA1) in co-culture. Experiments were repeated independently in 3 different subjects (3-8 cell culture replicates per subject) with similar results. Scale bar 30μm.

Supplementary Figure 6

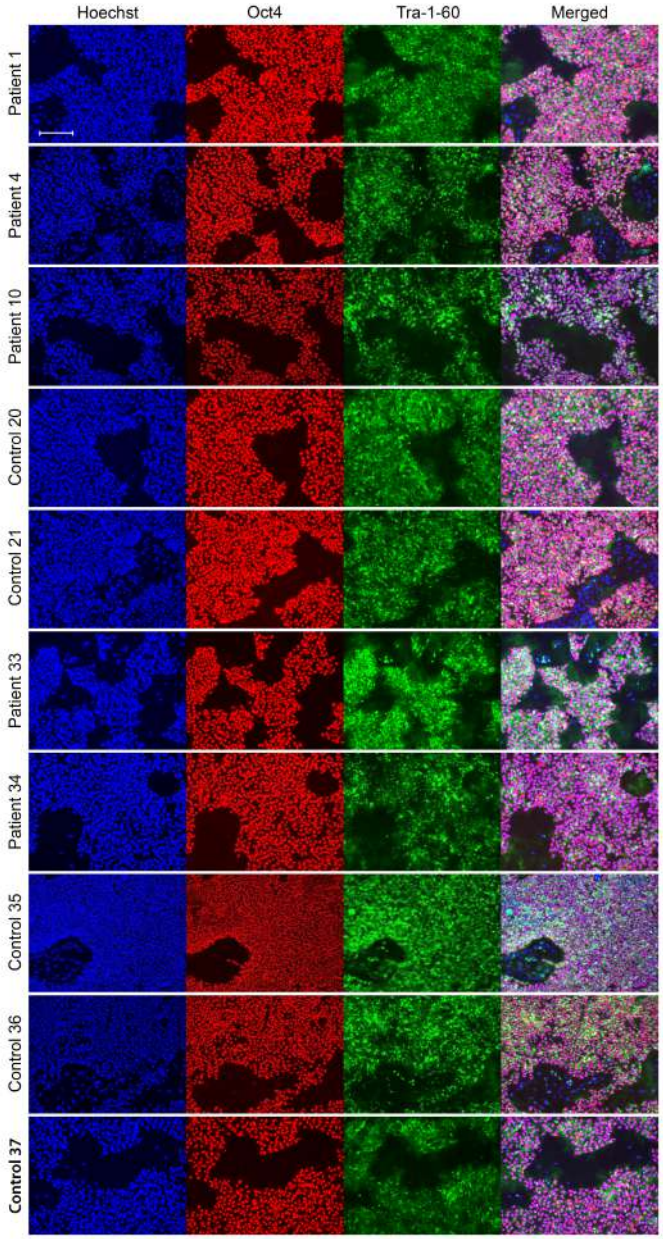

Supplementary Figure 6. Representative immunocytochemical characterization of pluripotent markers (OCT4, TRA 1-60) of control and patient-derived iPSC lines. Scale bar 100 μm. Experiments were repeated in eight independently iPSC-derivations across 8 subjects with similar results.

Supplementary Figure 7.

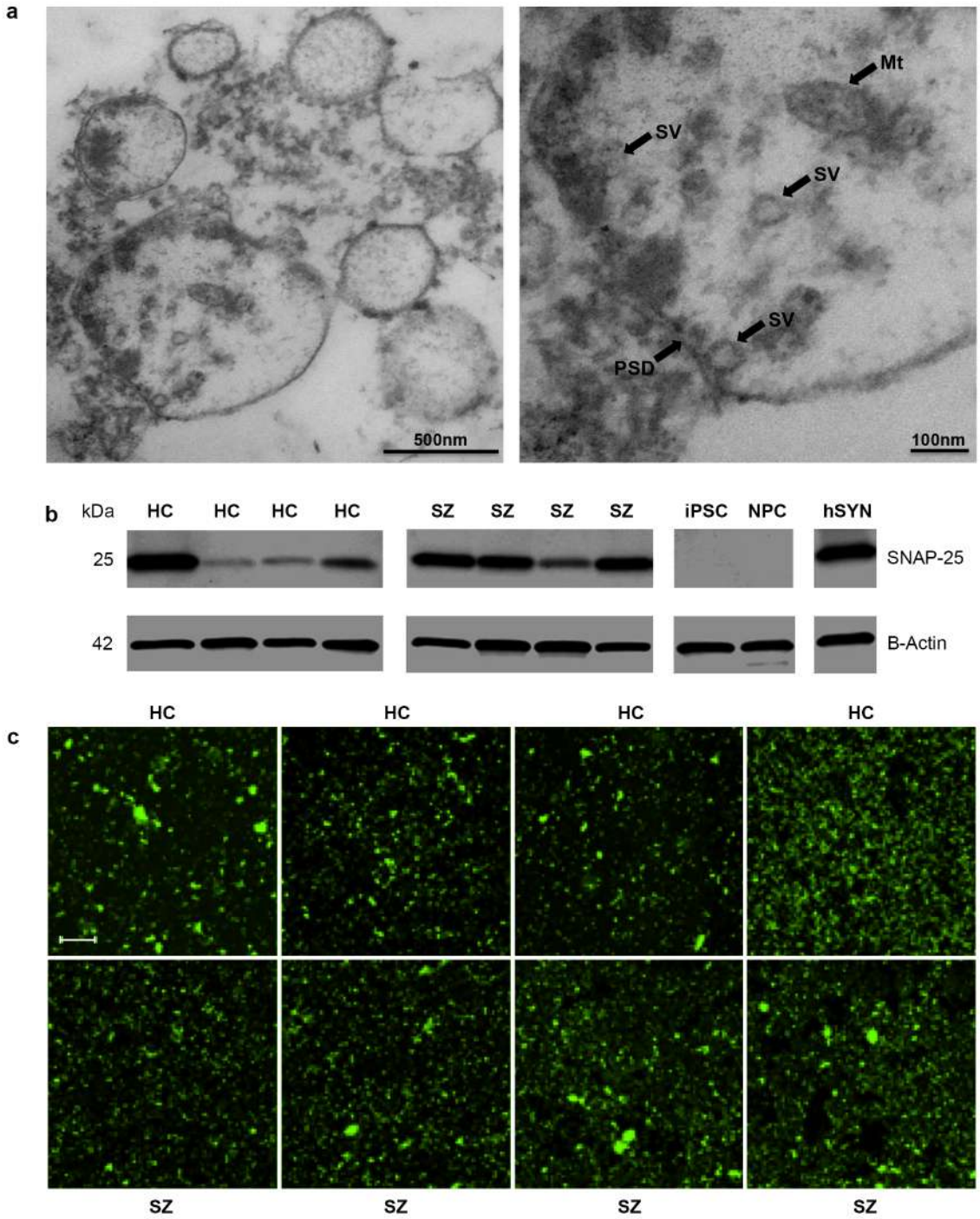

Supplementary Figure 7. (**a**)Transmission electron microscopy of isolated and fixed synaptosome suspensions examined at 60K (left) and 120K (right) magnification. Arrows indicate synaptic features PSD (post synaptic density), SV (synaptic vesicles) and Mt (mitochondria). Experiments were repeated independently in 2 different subjects (2 samples

per subject) with similar results. (**b**) Western analyses for the synaptic marker SNAP25 in synaptosome preparations. Lanes: 1-8, preparations from 4 healthy control (HC) and 4 schizophrenia (SZ) subjects in main analysis measuring phagocytic uptake of PSD-95 in induced microglia-like cells (iMGs). Lane 9, input iPSCs; lane 10, input NPCs; lane 11, post-mortem human brain synaptosome prep. We observed no significant difference in SNAP25 content (normalized to β-actin and in triplicates) between SZ subjects and HCs (Median: 0.54 [IQR: 0.15], HC: 0.42 [0.83], respectively, Mann-Whitney *U* test: P=0.94). Higher SNAP25 protein levels in synaptosome preparations did not predict higher phagocytic indexes ($r_{(spearman)}$= -0.12; P=0.78), nor did total protein levels (r_s= -0.36; P=0.12). (**c**) Representative images of the 4 SZ and HC synaptosome preparations showing $PSD95^+$ ICC staining. 40 randomly selected images per line were taken and automatically quantified using INCell Analyzer software. No difference in $PSD95^+$ counts could be observed on group level (HC median: 5884 [IQR; 5529], SZ median: 6511 [2516]; Mann-Whitney *U* test: P=0.69) umber of $PSD95^+$ particles per synaptosome preparations did not associate with uptake of $PSD95^+$ particles in our assays (r_s= -0.20; P=0.29). Scale bar 15 µm.

Supplementary Figure 8

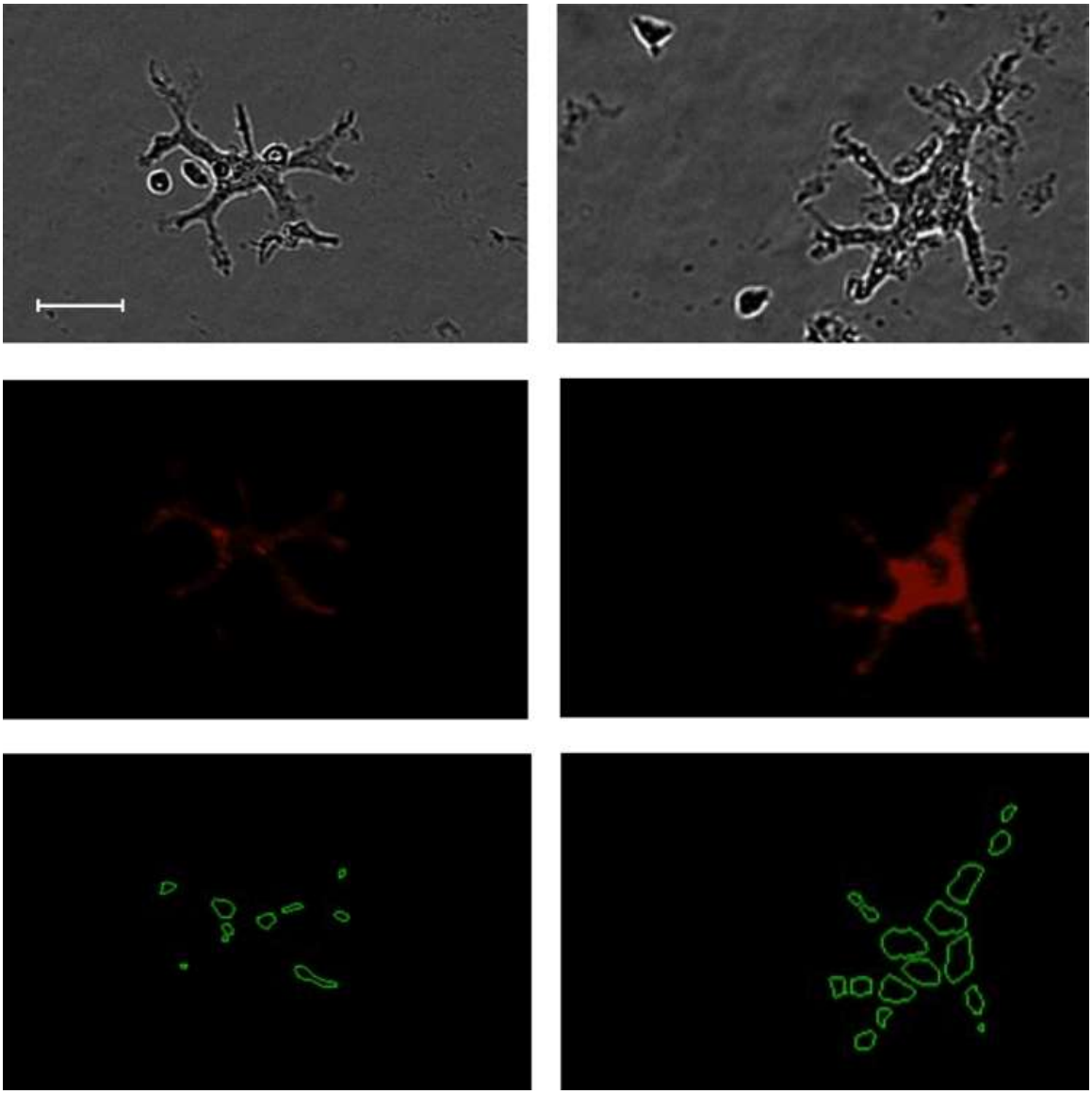

Supplementary Figure 8. Examples of pHrodo quantification in live imaging (from experiments described in Figure 3 and 4). Co-localization of phase contrast (top panels) and pHrodo labeling (middle panels) used to make masks (bottom panels) for quantification. Scale bar 20 µm.

Supplementary Figure 9

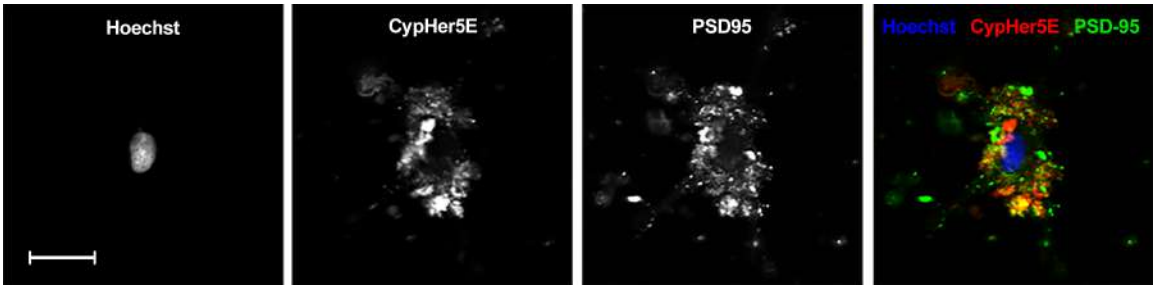

Supplementary Figure 9. Co-localization of CypHer5E™ and PSD-95^{+} puncta (confocal microscopy). Experiments were repeated independently in 2 different subjects (6 cell culture replicates per subject) with similar results. Scale bar 20 µm.

Supplementary Figure 10

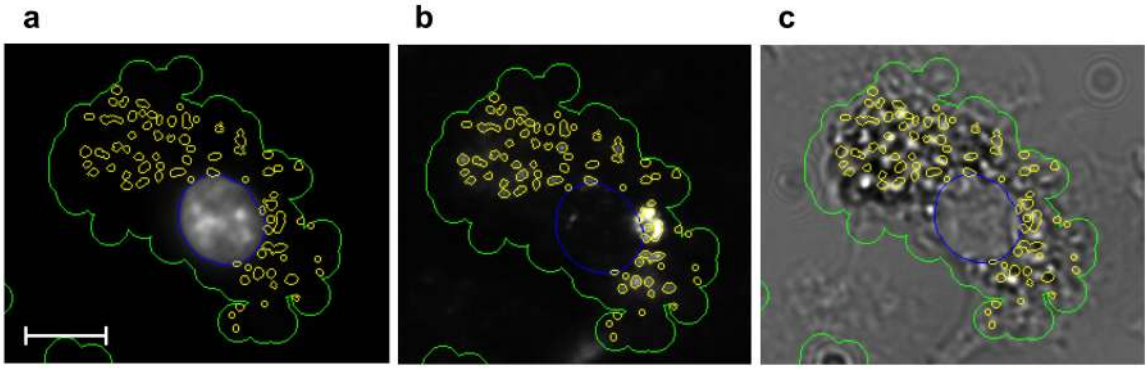

Supplementary Figure 10. Example of automated PSD-95^{+} puncta quantification using IN Cell Analyzer software (from experiments described in Figure 3 and 4). (**a)** Nuclear staining with software indicating cell outline (green) and PSD-95^{+} puncta (yellow). **(b)** PSD-95^{+} puncta staining with software indicating nucleus (blue), and cell outline (green). (**c**) Phase contrast image displaying same software indications. Scale bar 15 µm.

Supplementary Figure 11

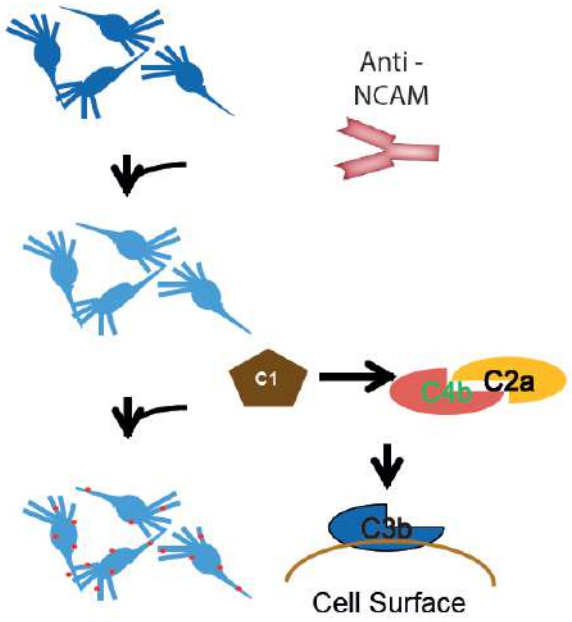

Supplementary Figure 11. Schematic of C3 deposition assay. Neuronal cultures are treated with an IgM anti-NCAM antibody to sensitize complement activation. Following antibody treatment, upstream complement components C1, C2 and C3 are supplemented. Because C4 is necessary for complement cascade activation, these conditions test the synthesis of C4 from the neuronal culture. Surface C3 deposition is measured with a fluorescent anti-C3 antibody, and anti-C3 immunofluorescence signal is normalized to anti-NCAM indirect immunofluorescence intensity.

Supplementary Figure 12

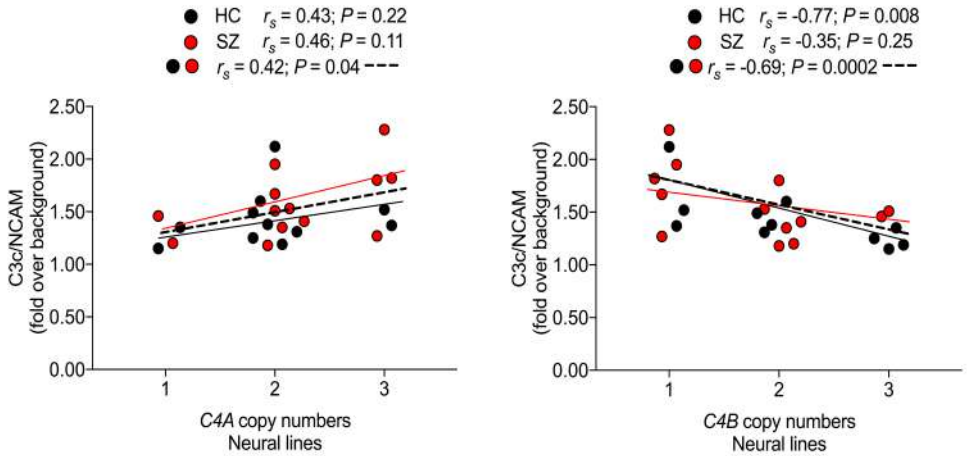

Supplementary Figure 12. Complement (C3) deposition on iPSC-derived neurons derived from 13 schizophrenia subjects (red dots) and 11 healthy first-degree relatives of these subjects (black dots) as an effect of *C4A* and *C4B* copy numbers. First, we treated the iPSC-derived neuronal cultures with an IgM anti-NCAM antibody to sensitize complement activation. Following antibody treatment, the upstream complement components C1, C2 and C3 were then supplemented. *C4A* and *C4B* copy numbers displayed a strong inverse correlation in both groups (HC: r_s = -0.76, P = 0.018, SZ: r_s = -0.62; P = 0.036). Correlation coefficients are Spearman's and p-values are two-sided.

Supplementary Figure 13.

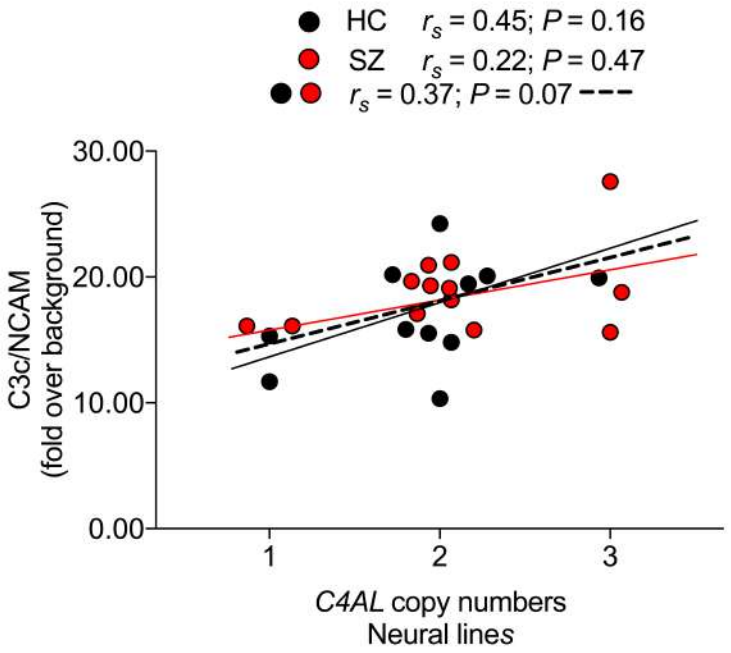

Supplementary Figure 13. Complement (C3) deposition (serum) on iPSC-derived neurons derived from 13 schizophrenia subjects (red dots) and 11 healthy first-degree relatives of these subjects (black dots) as an effect of *C4AL* copy numbers. First, we treated the iPSC-derived neuronal cultures with an IgM anti-NCAM antibody to sensitize complement activation. Following antibody treatment, 5 % C5-depleted serum was added. Correlation coefficients are Spearman's and p-values are two-sided.

Supplementary Figure 14.

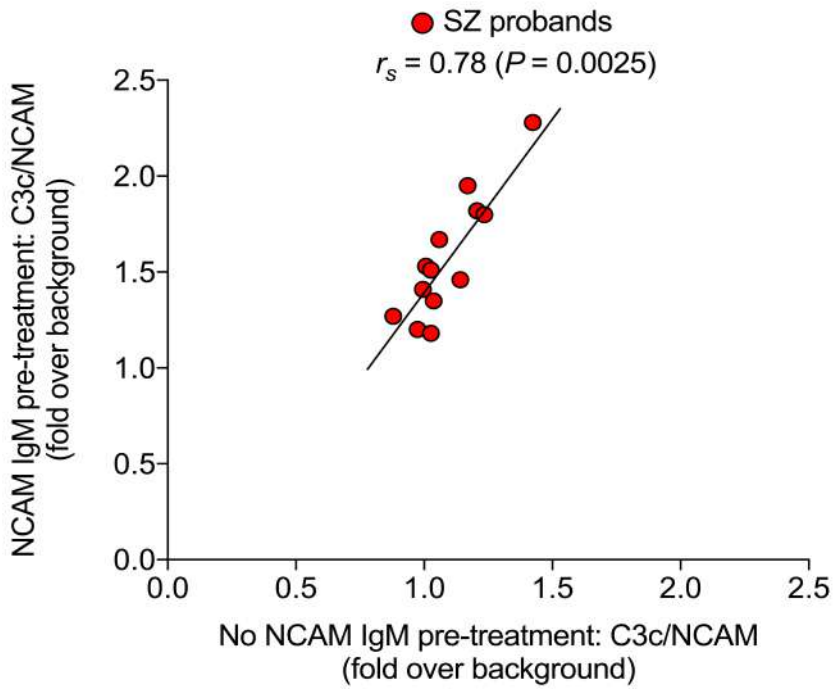

Supplementary Figure 14. Complement 3 **(**C3) deposition on human iPSC-derived neural cultures from 13 individuals with childhood-onset schizophrenia (see also Fig. 5a-d). We observed a strong correlation between C3 deposition with IgM anti-NCAM antibody pre-treatment (y-axis) and without (x-axis) with a more or less identical correlation between neural *C4AL* copy numbers (CN) and neural C3 complement deposition in experiments without IgM anti-NCAM pre-treatment (r_s = 0.64; P = 0.025) as in experiments using IgM anti-NCAM pre-treatment (r_s = 0.64; P = 0.017, see Fig 5a). Correlation coefficient is Spearman's and p-value is two-sided.

Supplementary Figure 15.

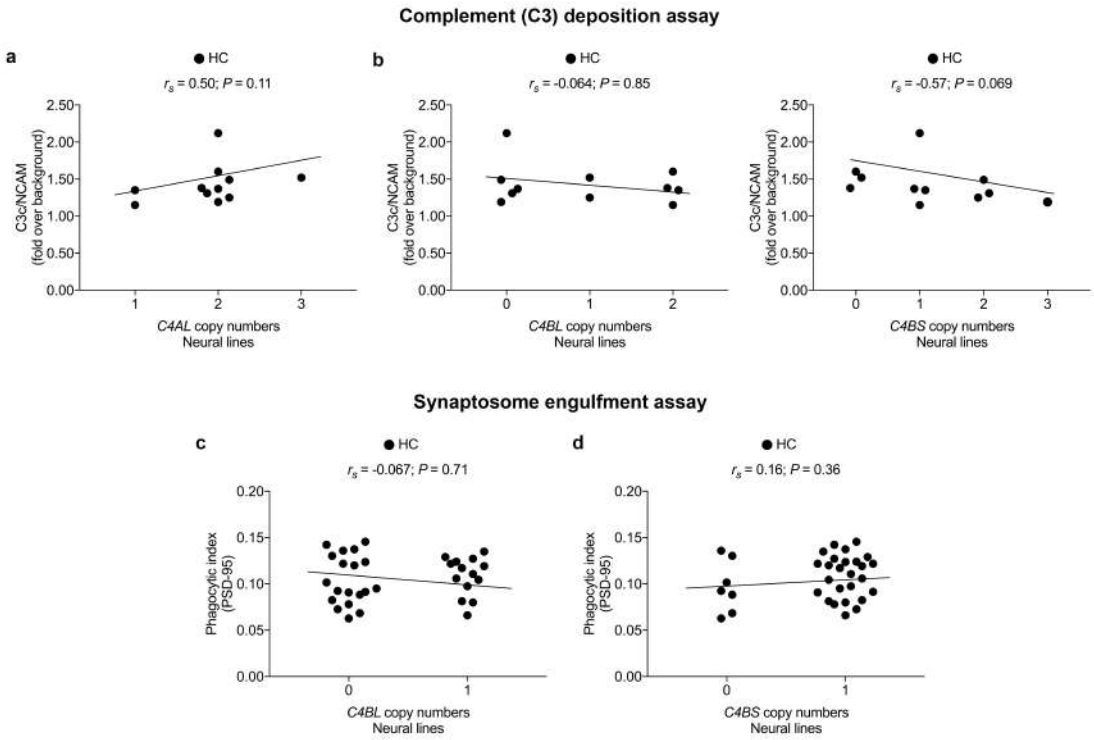

Supplementary Figure 15. (**a**) – (**b**) Complement (C3) deposition on iPSC-derived neurons derived from 11 healthy first-degree relatives (parents) of schizophrenia probands as an effect of different *C4AL, C4BL,* and *C4BS* copy numbers. iPSC-derived neuronal cultures with an IgM anti-NCAM antibody to sensitize complement activation. Following antibody treatment, the upstream complement components C1, C2 and C3 were then supplemented. (**c**) – (**d**) Phagocytic index (PSD-95+ inclusions) as a result of different *C4BL* and *C4BS* copy numbers among healthy controls contributing with iPSC-derived neural cultures for our synaptosome phagocytosis assay. Correlation coefficients are Spearman's and p-values are two-sided.

Supplementary Figure 16.

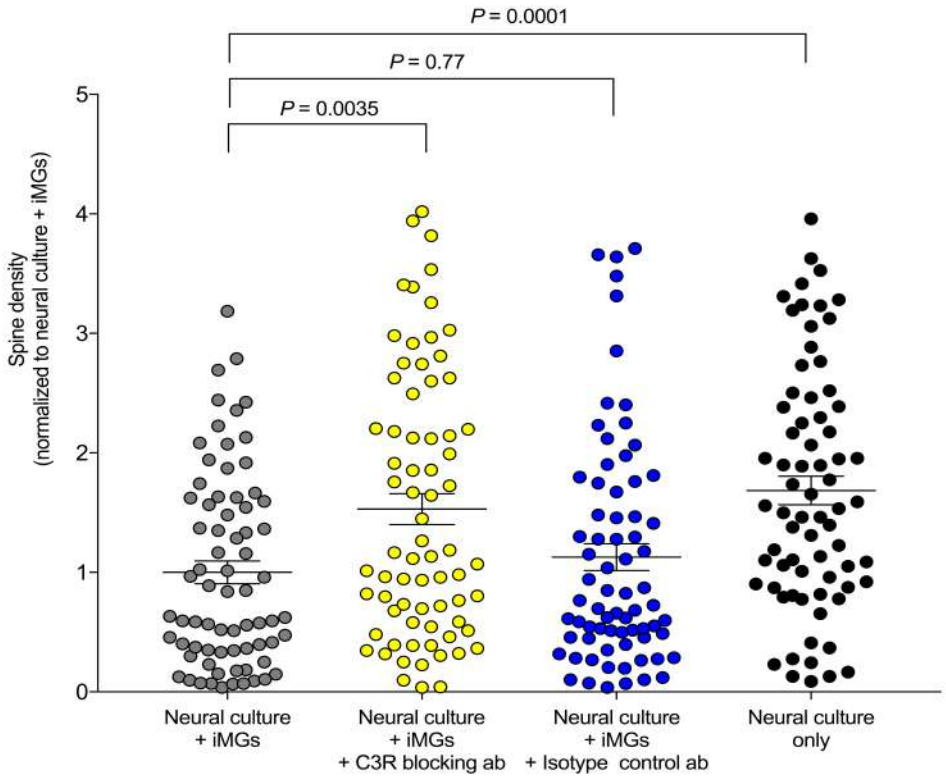

Supplementary Figure 16. Dendritic spine density as measured by spines per confocal microscopy image, normalized to counts in neural culture plus + microglia-like cells (iMGs) co-cultures (grey dots), of 2 schizophrenia subjects (n = 71 randomly selected dendrites). Yellow dots (n = 72) indicate dendritic spine density in co-cultures derived from same subjects but with pre-treatment using an anti-αM (clone M1/70) antibody in order to inhibit the microglia specific C3 receptor (C3R), while blue dots (n = 72) indicate pre-treatment with an isotype control antibody. Black dots (n = 72) indicate spine density in neural monocultures derived from same schizophrenia subjects. Error bars represent s.e.m and data was analyzed using an ANOVA ($F(3,283) = 7.95$; $P < 0.0001$) with the two-sided Sidak post test adjusted p-values are indicated in the graph ('neural culture + iMGs' as comparison group).

Supplementary Figure 17

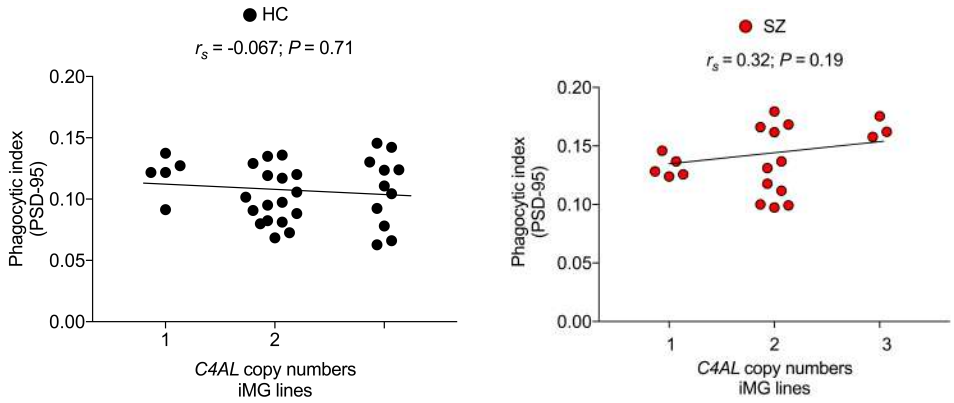

Supplementary Figure 17. Phagocytic index (PSD-95+ inclusions) as a result of different *C4AL* copy numbers among healthy controls (HC) and schizophrenia (SZ) subjects contributing with induced microglia-like cells (iMGs) for the synaptosome phagocytosis assay [n (HC – HC) = 33 models, n (SZ – SZ) = 19 models]. Correlation coefficients are Spearman's and p-values are two-sided.

Supplementary Figure 18.

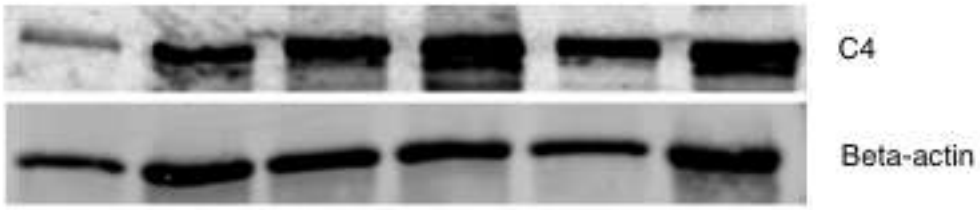

Supplementary Figure 18. Western blots of 6 isolated synaptosome preparations showing presence of C4.

Supplementary Figure 19

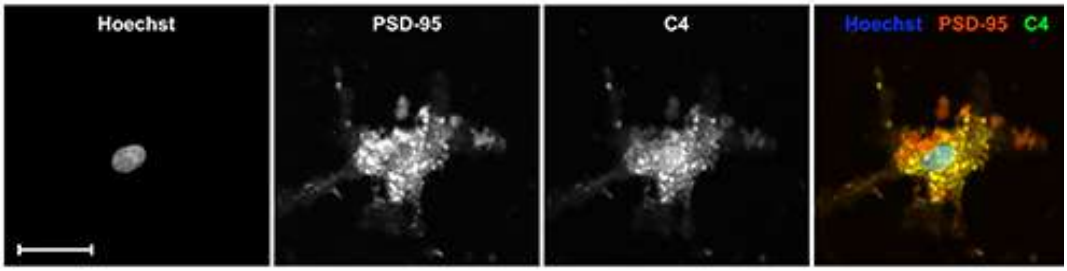

Supplementary Figure 19. Representative image of an induced microglia-like cell after treatment with synaptosomes that display co-localization of $C4^+$ puncta and PSD-95^+ puncta. Experiments were repeated independently in 6 different subjects (3-6 cell culture replicates per subject) with similar results. Scale bar 20 µm.

Supplementary Figure 20

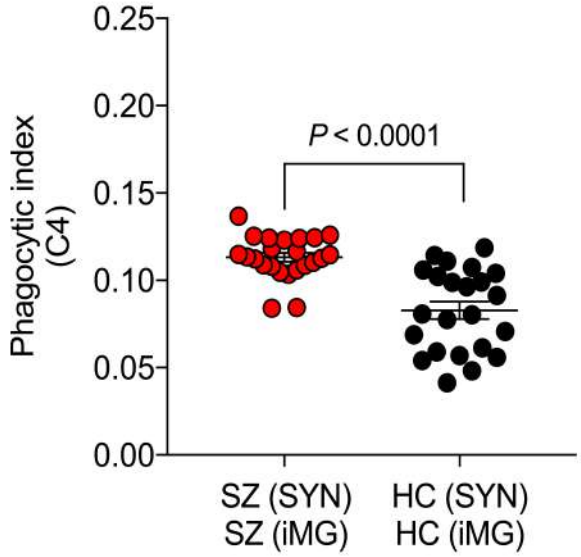

Supplementary Figure 20. Quantification (confocal microscopy) of phagocytic inclusions (C4+ inclusions, 0.5–1.5µm) in induced microglia-like cells (iMG) after exposure to synapstosomes. Red dot display n = 23 schizophrenia (SZ – SZ) models and black dots n = 23 healthy control (HC – HC) models. Data was analyzed using a *t*-test (Welch corrected): *t*-test(33.1) = 5.47 and reported p-value is two-sided. Mean ± s.e.m is indicated for each group.

Supplementary Figure 21

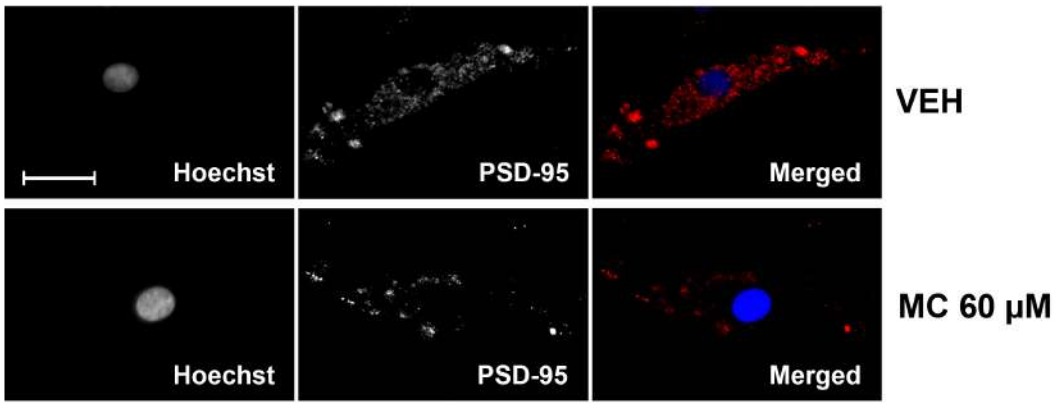

Supplementary Figure 21. Representative images displaying PSD-95^{+} phagocytic inclusions in iMGs 5.5 h after treatment with vehicle (VEH) or minocycline (MC; 60µM) of live imaging (confocal microscopy) from the experiments described in Figure 6. Scale bar 20 µm.

Supplementary Figure 22

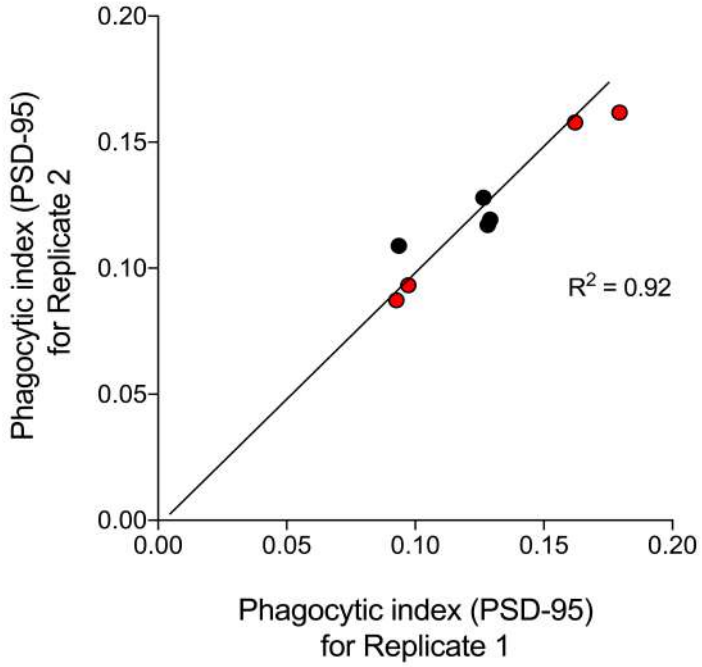

Supplementary Figure 22. Within-individual microglial assays in a patient vs. control setting and using different buffy coats. For 8 individuals (4 schizophrenia subjects [red dots] and 4 HCs [black dots]) microglia samples were derived from two different buffy coat samples. Each dot represent a pair of experiments with phagocytic index (PSD-95^{+} inclusions, 0.5–1.5µm, per iMG cytosol area) plotted on x-axis and y-axis for each replicate. Correlation between pairs (R-squared; Spearman) of samples was 0.92.

Supplementary Figure 23.

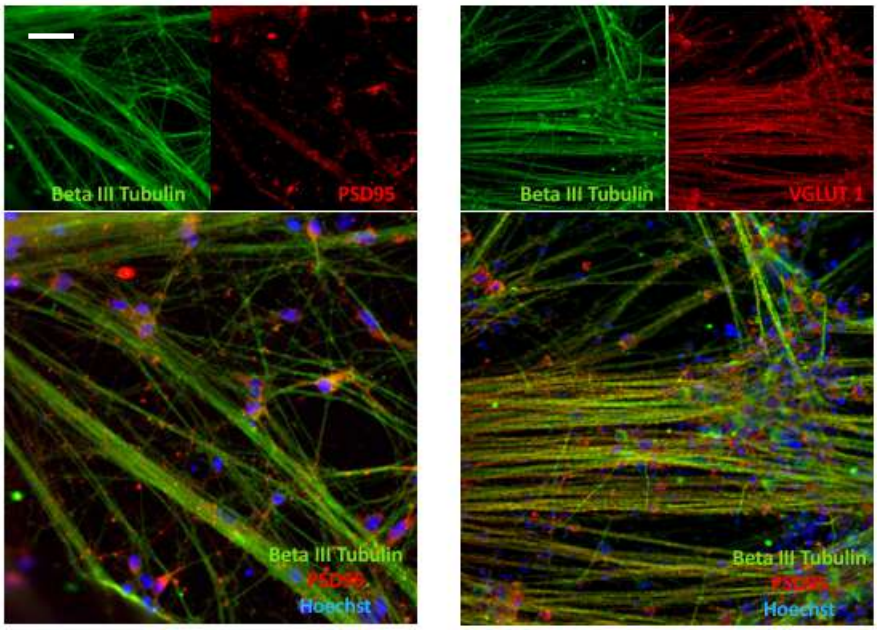

Supplementary Figure 23. Characterization of induced *NGN2* neurons used for co-cultures shows that a majority of the neurons are glutamatergic (VGLUT1^{+}) and express the post-synaptic marker PSD-95. Experiments were repeated independently in 3 different subjects (3-6 cell culture replicates per subject) with similar results. Scale bar: 100 µm.

Supplementary Figure 24.

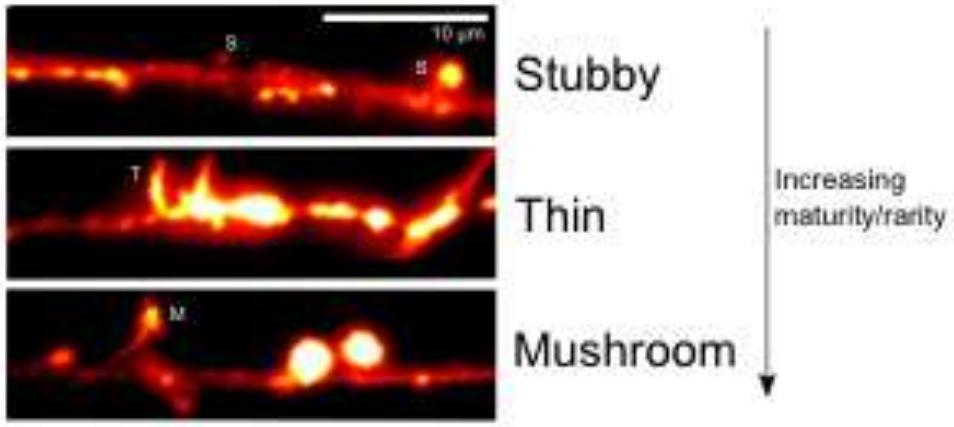

Supplementary Figure 24. Spine subtypes in induced *NGN2* neurons. Detailed spine analysis of images generated in experiments described in Figure 3 shows the presence of different sub-type of spines: thin, stubby and mushroom. Scale bar: 10 µm

Supplementary Table 1. Microglia-specific genes as defined by Bennett, M.L., *et al*. (2016).

TNFRSF1B; MIR4632; MIR7846	CD83	TFPI	NDUFC2-KCTD14; NDUFC2; KCTD14	CD300A
C1QA	MYLIP; MIR4639	SLC40A1	NDUFS3	SLC16A3; MIR6787
C1QC	SLC16A10	CMTM7	CTSD	RTN4RL1
C1QB	TREM2	ITGA9	LAG3	CXCL16
CD52	CD164	CCR5	NCKAP1L	STX8
CSF3R	SGK1	STAB1	TPCN1	SLC46A1
FAM102B	IFNGR1	CD86	P2RX7	ABHD15
CD53	SFT2D1	GP9	ORAI1	CCL3
CD53	TMEM14C	GPR160	C3AR1	CD79B
SCNM1; TNFAIP8L2	HFE	CMTM6	LDHB	SLC16A6
SLAMF8	FSCN1	DUSP7	CMKLR1	ABCA9
FCER1G	RAPGEF5	PROS1	TMEM119	CD68
SFT2D2	ELMO1	B4GALT4	SELPLG	LGALS9
CFH	SGCE	CD80	ITM2B	ITGB3
PTPRC	GAL3ST4	ITGB5	LPAR6	TTR
SRGAP2	LY96	P2RY13	KCTD12	TNFRSF11A
CR1L	ASPH	P2RY12	GPR183	TNFRSF11A
KLHL21	LY6E	LIPH	GAS6	LMAN1
SLC2A5	LY6E	UPK1B	PNP	GNA15
GPR157	TGFBR1	TLR9	ANG; RNASE4	EBI3
CNR2	TLR4	ETV5	EIF2S1	TBCB
PTAFR	RP11-281A20.2; TLR4	LAP3	GPR65	KCNK6
CSF3R	GOLM1	LAP3	KCNK13	CD37
ADORA3; TMIGD3	ENG	SMAD1	TMEM55B	TYROBP
NOTCH2	GPR34	TLR2	SLC7A7	TGFB1
SLC39A1	OPHN1	LOC101928877; RP11-386B13.3; SLC25A4	SLC7A8	LAIR1
DPM3	CYSLTR1	SLC25A4	NUMB	NDUFA3
FCRL1	SLC10A3	COMMD8	LGMN	NDUFA3
SLAMF9	TSPAN7	ABCG2	ASB2	NDUFA7
CD84	MRC1	CTSO	B2M	FAM110A
CD48	SLC29A3	TLR1	CD276	SIRPA
PVRL4	SLC29A3	TLR1	MPI	DYNLRB1
OLFML2B	ARHGAP12	TLR6	TSPAN3	SLCO4A1
CD34	BLNK	FAM105A	TMEM204	SLC17A9
TLR5	BLNK	HEXB	SNN	TGM2
DNAJB4	RGS10	CXXC5	TNFRSF17	SERINC3
OLFML3	ENTPD1	SEPP1	IL21R	STAU1
PLEKHO1	CD81	MEF2C	ITGAM	PMEPA1
F11R	POLR2G	TMEM173	ITGAM	IFNGR2
ITPRIPL1	FERMT3	CXXC5	DCTPP1	IFNGR2
MERTK	P2RY6	CD14	PYCARD	ITGB2
TMEM37	SLCO2B1	CSF1R	SERPINF1	RCAN1
ITGA6	THRSP	CD74	KCTD11	ITGB2
CASP8	IL10RA	SPARC	TRPV2	IFNAR2
SLC11A1	UBASH3B	LTC4S	CCL2	IL10RB
ADI1	SLC37A2	CD180	CCL4L2; CCL4; CCL4L1	COMT; MIR4761
TGFA	COMMD9	ECSCR	TMEM106A	CRYBA4
IL1A	ACP2	HAVCR2	G6PC3	CSF2RB
TMEM185B	ACVR1	SLC15A3	ABCC3	
LY86	GPR155	CTSF	TANC2	
OSM	PDGFB	CRYBB1	SYNGR1	

See Bennett, M.L., *et al.* (New tools for studying microglia in the mouse and human CNS. *Proc Natl Acad Sci U S A* **113**, E1738-1746 (2016)).

Supplementary Table 2. Microglia-specific genes as defined by Gosselin, D., *et al.* (2017)

TNFRSF1B; MIR4632; MIR7846	ARHGAP15	USP53	C2	VSIG4
RSC1A1; DDI2	DHRS9	TLR2	SERPINB9	EDA2R
C1QA	ANKRD44	TLR3	LOC100130357; RP1-257A7.4	IL2RG
C1QC	CASP10	CYTL1	HLA-DRB1	RP5-1091N2.9; IL2RG
C1QB	CASP8	SLC2A9	HLA-DMB	CYSLTR1
NCMAP	CTLA4	TLR10	HLA-DMA	BTK
RPS6KA1	SLC11A1	TMEM156	FAM46A	ELF4
RPS6KA1	CCL20	RBM47	RNASET2	ELF4
THEMIS2	SP140	PLAC8	SCIN	ATP11C
CSF3R	SP140L	HPSE	MYO1G	GAB3
ZC3H12A; MIR6732	SP100	HPGDS	IKZF1	ARHGAP4
PLK3	INPP5D	TIFA	LAT2	TMEM236
BTBD19	NLRC4	MAML3	NCF1	MRC1
CCDC18	OXER1	MAML3	PIK3CG	PLXDC2
CD53	ZFP36L2	TMEM154	CPED1	OTUD1
CD53	LOC100506142; RP11-417F21.1; RHOQ	TIGD4	IRF5	APBB1IP
C1orf162	PUS10	ZNF141	TBXAS1	MAP3K8
WNT2B	M1AP	ZNF141	TAS2R5	ALOX5
TTF2	MGAT4A	TLR1	GIMAP8	ALOX5
NBPF8	IL1A	TLR1	GIMAP2	WDFY4
FCGR1B	IL1B	TLR6	CARD11	TIMM23B
FCGR1A	TFCP2L1	GPRIN3	IGF2BP3	PALD1
HIST2H2AC	CYTIP	DDX60L	CPVL	PLAU
ADAMTSL4	LY75-CD302; CD302; LY75	DDX60L	AOAH	STAMBPL1
IL6R	DPP4	FAM105A	MYO1G	BTAF1
CD1D	DPP4	PTGER4	FGL2	HHEX
MNDA	ANKRD44	CARD6	ABCB4	SFXN2
IFI16	SP110	GAPT	SAMD9	NHLRC2
HSPA6	HTR2B	F2RL1	SAMD9L	VENTX
DUSP27	REL	S100Z	GAL3ST4	SFMBT2
SFT2D2	IL1RN	ERAP2	PIK3CG	LOC102724323; RP11-67C2.2; MARCH8
TBX19	NABP1	LNPEP	CREB3L2	C10orf128
C1orf112	ASXL2	ADRB2	CLEC5A	EGR2
FMO4	SNORD89; RNF149	DOCK2	ZNRF2	C10orf55
ZBTB37	RNF149	C5orf58	TFEC	ANKRD22
SOAT1	FANCD2	FYB	TFEC	CH25H
MR1	IRAK2	ANXA2R	TNFRSF10C	MYOF
NPL	TGFBR2	EMB	ADAM28	BLNK
OCLM	CMTM7	NAIP	POMK	BLNK
OCLM	ITGA9	LHFPL2	LY96	PIK3AP1
PLA2G4A	DLEC1	LNPEP	MYC	FFAR4
RGS18	CCR5	ST8SIA4	DENND3	CC2D2B
RGS1	CCRL2	TMEM173	DENND3	IL15RA
RGS2	FAM212A	CD14	PPP1R3B	AGAP5
PTPRC	UBA7	CSF1R	FGF20	KCNQ1
IKBKE	RASSF1-AS1	HAVCR1	FGL1	SLC22A18
TRAF3IP3	STAB1	DOCK2	REEP4	OR52N4
HLX	KBTBD8	KCNMB1	TNFRSF10B	RASSF10
FAM177B	EBLN2	HK3	TNFRSF10D	PDE3B
DISP1	ADPRH	DOK3	TNFRSF10A	PDE3B
NLRP3	CD86	DAB2	ADAM28	TMEM86A
CFAP74	PARP15	DAB2	RNF122	PRRG4
SLC2A5	PARP14	CD180	PLAG1	PTPRJ
IFNLR1	KBTBD12	NAIP	PAG1	FAM111A

PTAFR	ACPP	RAPGEF6	DPYS	MS4A4A
LAPTM5	SUCNR1	HAVCR2	SLA	FERMT3
COL8A2	GPR160	LCP2	MSR1	CCDC88B
CSF3R	SKIL	LY86	MSR1	CABP4
TCTEX1D4	B3GNT5	RREB1	DOCK8	FOLR2
FRRS1	ST6GAL1	GCNT2	JAK2	P2RY6
DENND2D	IL1RAP	CD83	JAK2	SLCO2B1
ADORA3; TMIGD3	IL1RAP	TRIM38	CD274	MYO7A
SYT6	LRCH3	HIST1H2BF	PDCD1LG2	RAB39A
CD58	FAM157A	HIST1H4E	MAMDC2	ATM
SRGAP2B	GHRL	HIST1H2AE	SYK	IL10RA
HIST2H2BF	SLC4A7	MICB	FGD3	SORL1
HIST2H2AB	CMTM6	TNF	SUSD3	SLC37A2
CTSS	GLB1; TMPPE	MSH5; MSH5-SAPCD1; SAPCD1	TGFBR1	KCNJ5
IL6R	XIRP1	HSPA1A; HSPA1B	TLR4	ST14
CD84	CX3CR1	HSPA1B; HSPA1A	RP11-281A20.2; TLR4	LMNTD2
ARHGAP30	CDCP1	HLA-DRA	CNTRL	TRIM22
FCGR3A	CCR1	HLA-DQA1	PTGS1	LYVE1
FCGR3B	UBA7; MIR5193	DEF6	C9orf106	SPI1
OLFML2B	CISH	FGD2	TOR4A	MPEG1
SELL	WNT5A	PTCRA	C9orf66	MS4A6A
SELL	WNT5A	RUNX2	BNC2	UNC93B1
TNFSF18	HCLS1	PRDM1	HACD4	KCNE3
NCF2	DZIP1L	TNFAIP3	B4GALT1	RAB38
FAM129A	P2RY13	STX11	ZCCHC6	CTSC
PTGS2	P2RY12	SUMO4	SYK	CASP4
NUAK2	IGSF10	SYTL3	FBP1	IL18
IL10	PLD1	HIST1H3D; HIST1H2AD	ABCA1	SORL1
TLR5	PLD1	HIST1H2BG	TNFSF8	C11orf45
ZNF124	KLHL6	IER3	ZBTB26	TRIM34
OLFML3	P3H2	HLA-DRB5	GBGT1	TRIM6-TRIM34
FCGR2A	ACKR2	HLA-DQB1	CARD9	TRIM22
FCGR2C	ZNF660	HLA-DOA	TLR7	MS4A7
IER5	NFKBIZ	HLA-DPA1	TLR8	MS4A14
MKNK1	NRROS	DEF6	CYBB	TCIRG1
TAL1	ZNF141	FKBP5	GPR34	FUT4
ADAMTSL4-AS1	SH3TC1	TREML1	WAS	BCO2; RPS12P21
EML4	N4BP2	TREM2	CLCN5	CASP1
PLEK	RHOH	PLA2G7	ATP7A	CD4
ARHGAP25	CEP135	MB21D1	DIAPH2	PTPN6
HK2	CXCL8	VNN2	DOCK11	CLEC2D
ITPRIPL1	BMP2K	SGK1	IL13RA1	TMEM52B
STEAP3	SPP1	IFNGR1	SOWAHD	PLBD1
KYNU	MMRN1	ZC3H12D	SASH3	KIAA1551
ARHGAP15	DAPP1	TAGAP	STK26	PCED1B
ARHGAP15	ALPK1	HFE	CXorf21	NCKAP1L
IRAK3; MIR6502	LPCAT2	LOC100129083; CTD-2616J11.2	TYMP; SCO2	RYR1
LYZ	CAPNS2	FPR2	ODF3B	CYP2S1
GLIPR1	NLRC5	KIR3DX1	RPS6KA1	FOSB
SH2B3	ADGRG5	FCAR	RPS6KA1	C5AR2
SH2B3	PLCG2	ZNF460	ZNF660	CD37
EP400NL	IRF8	C19orf35	RPS6KA1	RCN3
CACNA2D4	IGSF6	TMIGD2	RPS6KA1	SIGLEC16
LPAR5	SPN	ARRDC5	RPS6KA1	SIGLEC9
ACRBP	C16orf54	DENND1C	RPS6KA1	SIGLEC7
C3AR1	SNX20	C3	ZNF660	CD33
A2M	FHOD1	PRAM1	INPP5D	IL4R
CD69	DPEP2	MYO1F	RPS6KA1	APOBR
CLEC7A	ZFHX3	ZNF121	RPS6KA1	AC009133.17; C16orf54

OLR1	MLKL	LYL1	INPP5D	ITGAL
PLBD1	MAF	ADGRE2	INPP5D	PYCARD-AS1
ERP27	ITPRIPL2	RASAL3	RPS6KA1	ITGAM
BHLHE41	SPN	PLVAP	INPP5D	ITGAM
FAM60A	LOC100506388; RP11-1260E13.4; hosaru	JAK3	RPS6KA1	ITGAX
BIN2	SERPINF2	IL12RB1	RPS6KA1	ZNF267
ITGB7	SPNS3	LRRC25	INPP5D	ADCY7
GPR84	ZMYND15	LPAR2	RPS6KA1	PARVG
ARHGAP9	USP6	GMIP	FCGBP	CECR1
POC1B; POC1B-GALNT4; GALNT4	CCL4L2; CCL4; CCL4L1	ZNF100	INPP5D	CHEK2
IKBIP	CCL4L2; CCL4L1	CEBPA	ZNF660	OSM
CMKLR1	STAT5A	NFKBID	INPP5D	TNFRSF13C; MIR378I
TMEM119	TMEM106A	RASGRP4	INPP5D	NAGA
SELPLG	ABI3	MAP4K1	RPS6KA1	NFAM1
CLEC4A	MRC2	FCGBP	INPP5D	APOBEC3C
LRMP	MILR1	PLAUR	RPS6KA1	APOBEC3F
LRMP	CD300A	SLC1A5	INPP5D	APOBEC3G
HELB	SLC16A5	SIGLEC10	RPS6KA1	BCL2A1
OAS1	AANAT	SIGLEC8	RPS6KA1	IL16
FMNL3	TMC8	SIGLEC14; SIGLEC5	RPS6KA1	IL16
SPATA13; C1QTNF9	CARD14	FPR1	INPP5D	STARD5
ALOX5AP	RNF213	ZNF888	RPS6KA1	STARD5
LRCH1	SLC16A3; MIR6787	OSCAR	INPP5D	MSLN
ARL11	CXCL16	LAIR1	INPP5D	TNFRSF12A
TNFSF13B	SCIMP	TMEM150B	ZNF660	CIITA
ELF1	NLRP1	STXBP2	INPP5D	CLEC19A
ELF1	ASGR2	CEACAM21	RPS6KA1	ACSM5
ELF1	PIK3R6	APOC4	RPS6KA1	GRIK1-AS2; BACH1
ELF1	PIK3R5	APOC2	C19orf38	RUNX1
EPSTI1	TVP23C; CDRT4; TVP23C-CDRT4	APOC4-APOC2; APOC2	LYL1	RUNX1
LCP1	ABHD15	C5AR1	CLEC17A	RUNX1
LPAR6	SSH2	C5AR1	MVB12A; BISPR	IL17RA
KCTD12	EVI2A; EVI2B	ZNF808; RPL39P34	COLGALT1	HMOX1
ABCC4	SLFN12	LILRA2	PIK3R2; IFI30	NCF4
GPR183	CCL3	LILRA1	ZNF90	CSF2RB
TNFSF13B	CCL3L3; CCL3L1	LILRB1	ZNF85	CYTH4
TMEM255B	ARL5C	LILRB4	HAMP	CCDC134
ANG; RNASE4	ARHGAP27	LILRB4	KCNK6	CD93
RNASE6	GNGT2	ZNF846	RTTN	NFATC2
RNASE3	ERN1	ZNF846	RNF125	ZNF217
RNASE2	CD300LB	RGL3	LOC100505549; RP11-35G9.3	SIRPB2
RPGRIP1	CD300C	NUP62; IL4I1	DSC2	SIRPB1
MMP14	CD300LF	SIGLEC11	ARID3A	MX2
TSSK4	RHBDF2	ZNF600	EBI3	ITGB2
SUSD6	CEP295NL; TIMP2	ZNF816-ZNF321P	UHRF1	SAMSN1
GPR65	CD68	ZNF321P	VAV1	ITGB2
KCNK13	ADAP2	ZNF816	MYO1F	BACH1
PLD4	ITGB3	LILRB3	MYO1F	LIPC
TEP1	CLDN7	LILRA6	LRRK1	
SLC7A7	RNFT1	LILRB2	CYFIP1	
MIS18BP1	TBC1D3P1-DHX40P1	LILRA4	BMF	
PYGL	LIPG	SPTLC3	PLCB2	
PROX2	TNFRSF11A	HCK	PATL2	
SERPINA1	TNFRSF11A	TLDC2	ATP8B4	

GPR132	SOCS6	CASS4	SPPL2A	
LTB4R; LTB4R2	PSTPIP2	C20orf197	ADPGK	
RIPK3	CD226	SLC17A9	TBC1D2B	

See Gosselin, D.*, et al.* (An environment-dependent transcriptional network specifies human microglia identity. *Science* **356** (2017)).

Supplementary Table 3. Genes upregulated in induced microglia-like cells (iMGs) vs. monocytes.

Microglial genes from Bennett et al. 2016

Microglial genes from Gosselin et al. 2017

Microglial genes from Bennett et al. 2016 and Gosselin et al. 2017

Gene Symbol	Fold Change	P-value[1]	FDR P-value[2]	Affymetrix Probe ID
A2M	4126,69	1,35E-09	2,63E-06	TC0400008091.hg.1
ABCC3	3427,2	2,25E-10	1,20E-06	TC1000006911.hg.1
ACP2	2149,99	7,52E-09	6,72E-06	TC1400008705.hg.1
ADAP2	1436,85	8,79E-11	9,42E-07	TC2000007514.hg.1
ALOX5AP	1329,46	2,79E-08	1,46E-05	TC0700006913.hg.1
ANKRD22	1231,06	3,50E-07	5,44E-05	TC1000006912.hg.1
ASPH	1126,9	2,05E-07	4,02E-05	TC1900011759.hg.1
ATP8B4	1059,16	5,75E-10	1,77E-06	TC1000010273.hg.1
BHLHE41	903,97	3,71E-10	1,59E-06	TC1700009850.hg.1
BLNK	868,71	7,94E-09	6,81E-06	TC0300014082.hg.1
BMP2K	791,48	5,27E-07	6,69E-05	TC1700007557.hg.1
C1QA	776,12	1,29E-09	2,63E-06	TC2000009250.hg.1
C1QB	769,22	2,60E-08	1,46E-05	TC1100008453.hg.1
C1QC	647,07	2,89E-06	0,0002	TC1900008669.hg.1
C2	634,47	2,74E-08	1,46E-05	TC0500010615.hg.1
C3	589,68	4,37E-08	1,93E-05	TC1700007561.hg.1
C3AR1	522,06	2,30E-08	1,40E-05	TC0100016983.hg.1
CASP8	482,62	4,10E-08	1,87E-05	TC1800007850.hg.1
CCL2	457,71	0,0001	0,0017	TC0100018551.hg.1
CCL3	448,53	5,35E-06	0,0003	TC0700012849.hg.1
CCL3L3; CCL3L1	445,75	6,84E-09	6,38E-06	TC1200012749.hg.1
CCR1	355	7,03E-07	7,73E-05	TC1400008606.hg.1
CCR5	310,04	2,10E-09	3,36E-06	TC0100010269.hg.1
CD14	287,66	5,27E-05	0,0011	TSUnmapped00000392.hg.1
CD274	287,44	6,07E-06	0,0003	TC1400010012.hg.1
CD53	283,82	0,0003	0,0041	TC1100012134.hg.1
CD84	255,5	1,05E-06	9,49E-05	TC2000008279.hg.1
CDCP1	233,94	3,05E-09	3,44E-06	TC0100014014.hg.1
CECR1	229,64	9,97E-08	3,19E-05	TC1200009847.hg.1
CH25H	215	7,82E-07	8,18E-05	TC0100014276.hg.1
CLEC5A	200,37	9,50E-07	9,20E-05	TC0100013369.hg.1
CMKLR1	197,23	3,00E-08	1,52E-05	TC0200010545.hg.1
CSF1R	178,67	9,96E-08	3,19E-05	TC0200007296.hg.1
CSF3R	169,94	2,26E-07	4,25E-05	TC0300013520.hg.1

CXCL8	157,87	5,42E-06	0,0003	TC0800012389.hg.1
CYTIP	138,45	2,85E-09	3,44E-06	TC1400010616.hg.1
DAB2	122,79	2,37E-09	3,39E-06	TC1000011585.hg.1
DENND3	121,92	4,43E-07	6,20E-05	TC0100016199.hg.1
EGR2	120,56	2,84E-06	0,0002	TC0X00009911.hg.1
ELF1	115,99	7,01E-08	2,64E-05	TC0600012434.hg.1
ELF4	113,61	2,84E-06	0,0002	TC1100013161.hg.1
ERN1	112,1	1,89E-07	4,02E-05	TC0200015578.hg.1
ETV5	108,92	1,22E-07	3,37E-05	TC0600011953.hg.1
FAM46A	105,54	5,39E-06	0,0003	TC1000008643.hg.1
FBP1	104,86	9,94E-08	3,19E-05	TC0300007437.hg.1
FCAR	104,65	0,0012	0,0102	TC1500009738.hg.1
FCGBP	102,99	1,29E-05	0,0004	TC1200011838.hg.1
FCGBP	102,51	6,68E-10	1,77E-06	TC0100009364.hg.1
FCGR1A	98,01	2,40E-06	0,0002	TC0700013471.hg.1
FCGR3A	97,74	0,0009	0,0079	TC0100016952.hg.1
FCGR3B	92,09	7,89E-06	0,0003	TC1900009443.hg.1
FOLR2	89,08	1,63E-05	0,0005	TC0X00007039.hg.1
FOSB	89,05	0,0005	0,0051	TC1000011376.hg.1
G6PC3	88,6	5,04E-09	5,02E-06	TC0100011953.hg.1
GPR34	79,97	3,87E-09	4,15E-06	TC1600009683.hg.1
HLA-DQA1	79,32	3,41E-06	0,0002	TC1800008285.hg.1
HPGDS	77,88	2,97E-09	3,44E-06	TC1600010752.hg.1
IER5	75,45	7,24E-07	7,84E-05	TC0200013265.hg.1
IGSF6	74,27	1,03E-08	8,22E-06	TC0400010465.hg.1
IL10RA	72,96	4,69E-05	0,001	TC0100007292.hg.1
INPP5D	72,75	0,0001	0,0019	TC0100007291.hg.1
IRF8	70,72	0,0009	0,008	TC1600007235.hg.1
ITGB3	67,22	7,22E-06	0,0003	TC1200011845.hg.1
LAIR1	66,8	0,0054	0,0316	TC0600007377.hg.1
LGMN	64,79	2,88E-07	4,84E-05	TC0300014095.hg.1
LHFPL2	64,7	1,61E-05	0,0005	TC0100010100.hg.1
LMAN1	62,86	2,11E-05	0,0006	TC0300011173.hg.1
LPCAT2	62,77	0,0016	0,0125	TC0400007344.hg.1
LRMP	62,45	1,76E-05	0,0005	TC0100010874.hg.1
LY96	60,9	0,0003	0,0035	TC1300007794.hg.1
MAF	60,63	5,15E-09	5,02E-06	TC1000012542.hg.1
MERTK	60,48	1,90E-06	0,0001	TC1200010977.hg.1
MMP14	58,09	0,0003	0,0037	TC1200012748.hg.1
MRC1	58,05	2,35E-08	1,40E-05	TC1700007016.hg.1
MS4A4A	57,82	2,73E-07	4,76E-05	TC1800006589.hg.1
MSR1	57,59	2,23E-05	0,0006	TC0400011348.hg.1
MYO1G	57,33	1,01E-06	9,30E-05	TSUnmapped00000244.hg.1

NLRC5	57,26	1,54E-07	3,93E-05	TC0600011771.hg.1
NLRP3	57,06	0,0003	0,0036	TC0100013305.hg.1
NPL	56,84	0,0006	0,0063	TC0200015650.hg.1
OAS1	55,88	1,81E-07	4,02E-05	TC0100010454.hg.1
OLFML2B	54,49	3,88E-07	5,77E-05	TC1100010946.hg.1
P2RX7	54,19	2,21E-06	0,0001	TC1400008689.hg.1
PDCD1LG2	53,97	6,09E-07	7,18E-05	TC0500012455.hg.1
PIK3R1	53,59	6,05E-07	7,18E-05	TC0500013301.hg.1
PLA2G7	53,46	2,10E-05	0,0006	TC0600009381.hg.1
PLAU	53,44	1,72E-08	1,19E-05	TC0400007938.hg.1
REL	52,15	3,27E-06	0,0002	TC0300010913.hg.1
RGS18	51,97	3,97E-06	0,0002	TC0100014769.hg.1
RGS2	51,2	2,34E-06	0,0002	TSUnmapped00000484.hg.1
RUNX2	51,19	0,0004	0,0043	TC1800007508.hg.1
SAMD9L	51,08	1,33E-08	9,81E-06	TC1200010182.hg.1
SELPLG	50,27	4,23E-07	6,17E-05	TC1600010951.hg.1
SEPP1	48,75	7,76E-06	0,0003	TC0800008467.hg.1
SH2B3	48,34	2,19E-06	0,0001	TC1000008234.hg.1
SLAMF8	48,06	0,0003	0,0033	TC0500012247.hg.1
SLC17A9	47,21	2,85E-07	4,84E-05	TC1100010730.hg.1
SLC29A3	46,41	3,84E-06	0,0002	TC0300014092.hg.1
SLC37A2	44,77	1,76E-06	0,0001	TC1100012510.hg.1
SLC39A8	43,95	8,85E-06	0,0003	TC0100013561.hg.1
SLCO2B1	43,61	1,29E-06	0,0001	TC1700007560.hg.1
SPATA13; C1QTNF9	41,43	1,85E-08	1,24E-05	TC1100006500.hg.1
SPP1	41	0,0001	0,0022	TC2000007519.hg.1
STX11	40,25	1,34E-05	0,0005	TC0100007290.hg.1
TFEC	39,66	9,69E-07	9,20E-05	TC0200010713.hg.1
TMEM106A	39,56	5,52E-05	0,0011	TC0500007138.hg.1
TMEM14C	39,14	2,16E-06	0,0001	TC0900009513.hg.1
TMEM154	38,84	5,63E-07	6,98E-05	TC0900006937.hg.1
TMEM236	38,11	5,20E-06	0,0002	TC0200009065.hg.1
TNFAIP3	37,9	0,0001	0,0018	TC0300008242.hg.1
TNFRSF11A	37,69	1,93E-06	0,0001	TC0500008483.hg.1
TNFRSF11A	37,66	4,77E-08	2,01E-05	TC0800010766.hg.1
TNFRSF1B; MIR4632; MIR7846	37	2,63E-07	4,67E-05	TC0300007485.hg.1
TREM2	36,65	1,61E-07	3,96E-05	TC1700011045.hg.1
TREML1	36,59	1,14E-06	9,85E-05	TC0200008894.hg.1
TRPV2	35,44	6,57E-07	7,53E-05	TC1000012577.hg.1
VSIG4	35,32	3,86E-05	0,0009	TC1200009157.hg.1
ZC3H12A; MIR6732	35,04	1,75E-07	4,00E-05	TSUnmapped00000300.hg.1

AAAS	34,87	4,91E-08	2,02E-05	TC1200009735.hg.1
AAMDC	34,49	1,12E-05	0,0004	TC1700010358.hg.1
AARS	34,34	1,50E-06	0,0001	TC1200010145.hg.1
ABCD3	34,27	0,005	0,0296	TC1000012235.hg.1
ACACA	34,21	3,45E-06	0,0002	TC0100008126.hg.1
ACKR3	34,08	1,06E-07	3,26E-05	TC0200013095.hg.1
ACO1	33,62	2,22E-06	0,0001	TC0700009061.hg.1
ADAM17	33,55	2,08E-05	0,0006	TC1000009851.hg.1
ADM	33,51	2,39E-05	0,0006	TC0500006730.hg.1
ADRBK1	33,33	2,05E-05	0,0006	TC1400006659.hg.1
AGTPBP1	33,3	5,41E-05	0,0011	TC0600007664.hg.1
AHCTF1	33,07	2,99E-05	0,0007	TC1000010276.hg.1
AKR1A1	33,07	4,51E-08	1,93E-05	TC1800007667.hg.1
ALCAM	32,7	3,81E-07	5,77E-05	TC0100016189.hg.1
ALG1L2	32,34	3,55E-06	0,0002	TC0900010866.hg.1
AMBRA1	31,72	8,27E-05	0,0015	TC0700011797.hg.1
AMPD2	31,18	1,31E-05	0,0004	TC0100012167.hg.1
ANAPC7	30,86	1,78E-05	0,0005	TC0900008716.hg.1
ANKDD1A	30,54	5,66E-08	2,25E-05	TC0200015476.hg.1
ANKH	30,31	3,90E-06	0,0002	TC0900006560.hg.1
ANLN	30,21	0,0103	0,0517	TC0700007198.hg.1
ANOS1	30,02	5,69E-05	0,0011	TC0900012167.hg.1
ANXA2	29,89	3,66E-05	0,0009	TC0900006559.hg.1
ANXA4	29,82	5,51E-08	2,23E-05	TC0300013866.hg.1
ANXA4	29,76	4,43E-07	6,20E-05	TC1300008533.hg.1
AP2A2	29,49	8,77E-05	0,0015	TC0600011124.hg.1
APOA2	29,43	3,63E-08	1,73E-05	TC0100016917.hg.1
APOBEC3A	29,27	1,66E-07	4,00E-05	TC0100010855.hg.1
APOC1	29,12	2,21E-05	0,0006	TC0500011225.hg.1
ARHGAP18	28,39	2,31E-05	0,0006	TC0200010410.hg.1
ARHGAP31	28,15	0,0007	0,0064	TC1800006448.hg.1
ARHGEF9; ARHGEF9-IT1	27,7	2,30E-05	0,0006	TC0300008467.hg.1
ARID3B	27,67	0,0004	0,0045	TC1500007392.hg.1
ARL4A	27,62	3,04E-08	1,52E-05	TC2000008237.hg.1
ARL4C	27,2	2,47E-05	0,0007	TC1700010459.hg.1
ARL8A	27,06	2,60E-05	0,0007	TC0900007863.hg.1
ARRDC3	26,92	1,71E-07	4,00E-05	TC0400007556.hg.1
ARV1	26,72	4,91E-06	0,0002	TC0100016018.hg.1
ATF3	26,62	4,08E-06	0,0002	TC0100011267.hg.1
ATG2A	26,57	0,0012	0,0101	TC1100009408.hg.1
ATG9A	26,44	3,07E-05	0,0008	TC0100016135.hg.1
ATIC	26,4	6,34E-08	2,47E-05	TC1000011515.hg.1
ATL2	26,2	7,62E-07	8,13E-05	TC0200012072.hg.1

ATP10D	25,82	1,79E-05	0,0005	TC1000007954.hg.1
ATP2A3	25,7	0,0065	0,0364	TC0600007657.hg.1
ATP2B4	25,49	0,0021	0,0156	TC0400011920.hg.1
ATP5G3	25,47	0,0046	0,0279	TC1000011368.hg.1
ATP5J2	25,29	0,0005	0,0053	TC0100011770.hg.1
ATP6V1C1	25,03	1,57E-07	3,95E-05	TC0200016584.hg.1
ATRN	24,68	0,0027	0,0184	TC1200008597.hg.1
AURKB	24,61	2,02E-06	0,0001	TC1000007698.hg.1
BANF1	24,49	2,79E-05	0,0007	TC0100014408.hg.1
BARD1	24,16	8,63E-05	0,0015	TC0700010247.hg.1
BBX	24,1	4,54E-07	6,20E-05	TSUnmapped00000777.hg.1
BCAT1	24,03	5,19E-07	6,66E-05	TSUnmapped00000138.hg.1
BCL11A	24	1,69E-07	4,00E-05	TC0400007422.hg.1
BCL2L11	23,7	4,47E-06	0,0002	TC0700006567.hg.1
BCL3; MIR8085	23,55	1,81E-07	4,02E-05	TC0100016185.hg.1
BCL7B	23,43	1,20E-07	3,37E-05	TC1600007931.hg.1
BCLAF1	23,42	0,0012	0,0105	TC0800009619.hg.1
BCOR	23,27	9,18E-05	0,0016	TC1200009807.hg.1
BLVRB	23,17	1,17E-05	0,0004	TC1200009300.hg.1
BMP6	22,85	0,0036	0,0231	TC1100013022.hg.1
BOLA3	22,69	9,25E-07	9,10E-05	TC0700012968.hg.1
BRI3BP	22,68	6,98E-05	0,0013	TC0200015893.hg.1
BTBD9	22,59	0,0156	0,071	TC0300007324.hg.1
C10orf54	22,56	9,34E-07	9,15E-05	TC2100008314.hg.1
C11orf73	22,35	5,15E-06	0,0002	TC0300007257.hg.1
C14orf1	22,28	4,88E-06	0,0002	TC0800007086.hg.1
C14orf119	22,23	1,27E-05	0,0004	TC0400008004.hg.1
C15orf39	22,12	8,96E-05	0,0015	TC0600011870.hg.1
C16orf62	21,9	6,76E-08	2,59E-05	TC1700007976.hg.1
C16orf72	21,85	1,16E-06	9,96E-05	TC1700012126.hg.1
C16orf87	21,68	1,91E-06	0,0001	TC1700012226.hg.1
C17orf62	21,5	2,85E-05	0,0007	TSUnmapped00000077.hg.1
C18orf25	21,41	3,81E-06	0,0002	TC1200012666.hg.1
C21orf59	21,15	1,27E-07	3,41E-05	TC1400010757.hg.1
C2orf88	21,06	8,02E-07	8,27E-05	TC0700013468.hg.1
C6orf191andARHGAP18; RP1-69D17.4; RP1-69D17.3; TCONS_l2_00025470; TCONS_l2_00024911; LAMA2	21,05	0,0004	0,0043	TC0300010943.hg.1
CALU	21,04	3,07E-07	4,99E-05	TC0700013609.hg.1
CAMK1	20,99	1,02E-07	3,20E-05	TC0300013852.hg.1

CAMP	20,68	0,0004	0,0048	TC1100008341.hg.1
CAPG	20,66	1,21E-06	0,0001	TC2100007032.hg.1
CARD19	20,58	0,0007	0,0071	TC0400011748.hg.1
CBR1	20,53	0,0077	0,0414	TC1700008228.hg.1
CCDC126	20,34	0,0003	0,0036	TC0400012949.hg.1

[1]Two-sided p-values derived from one-way ANOVAs. [2]False discovery rate adjusted p-values. Monocytes were derived from 2 subjects (3 samples; n = 6) and induced microglia-like cells from 3 subjects (3 samples; n = 9). Only genes upregulated with a fold change > 20 are included in the table.

Supplementary Table 4. Genes upregulated in induced microglia-like cells (iMGs) vs. monocyte-derived macrophages.

Microglial genes from Bennett et al 2016
Microglial genes from Gosselin et al 2017
Microglial genes from Bennett et al 2016 and Gosselin et al 2017

Gene Symbol	Fold Change	P-value[1]	FDR P-value[2]	Affymetrix probe ID
CCL13	754,76	1,02E-08	6,61E-05	TC1700007561.hg.1
CD163	666,99	1,83E-09	3,93E-05	TC1200012749.hg.1
CLEC5A	495,02	4,63E-06	0,0014	TC0700012849.hg.1
FCGBP	340,67	1,99E-05	0,0035	TSUnmapped00000392.hg.1
RNASE1	274,28	3,89E-07	0,0003	TC1400008606.hg.1
MS4A6A	271,19	1,11E-07	0,0001	TC1100010996.hg.1
ANKRD22	247,75	8,05E-05	0,0086	TC1000011368.hg.1
COLEC12	206,22	5,23E-08	0,0001	TC1800007850.hg.1
CLDN1	191,89	6,74E-08	0,0001	TC0300013520.hg.1
PPBP	179,89	2,19E-08	7,82E-05	TC0400011013.hg.1
TGFBI	163,73	9,09E-06	0,0021	TC0500008736.hg.1
CH25H	146,72	0,0001	0,0102	TC1000011376.hg.1
CD14	114,21	2,16E-05	0,0037	TC0500012247.hg.1
TMEM236	112,65	1,94E-08	7,82E-05	TC1000006911.hg.1
CCL2^	107,81	5,08E-06	0,0014	TC1700007557.hg.1
TREM1	105,25	2,59E-06	0,0009	TC0600011777.hg.1
PMP22	98,63	6,19E-09	6,61E-05	TC1700009850.hg.1
SEPP1	92,45	1,25E-07	0,0001	TC0500010615.hg.1
FPR3	83,87	7,03E-05	0,0079	TC1900008669.hg.1
OLFML2B	75,54	7,84E-07	0,0004	TC0100016199.hg.1
C3AR1	72,81	2,23E-06	0,0009	TC1200009807.hg.1
FCGR2C	67,85	3,02E-06	0,001	TC0100018309.hg.1
C1QC	66,87	7,12E-05	0,0079	TC0100007291.hg.1
IL7R	64,78	2,18E-05	0,0037	TC0500007138.hg.1
FCGR2B	63,42	0,0004	0,0243	TC0100018310.hg.1
ETV5	61,57	2,43E-07	0,0002	TC0300014082.hg.1
FCGR2A	57,46	1,91E-07	0,0002	TC0100018308.hg.1
AIF1	51,74	6,72E-08	0,0001	TC0600007598.hg.1
MGAM	48,32	4,99E-06	0,0014	TC0700013471.hg.1
CCL8	44,65	4,32E-07	0,0003	TC1700007560.hg.1
GPR34	43,95	1,00E-05	0,0023	TC0X00007039.hg.1
SLCO2B1	40,61	1,43E-06	0,0006	TC1100008453.hg.1
CMKLR1	39,13	4,72E-05	0,0059	TC1200011838.hg.1
MEF2C	37,28	2,59E-06	0,0009	TC0500011418.hg.1
STAB1	34,15	1,36E-06	0,0006	TC0300007484.hg.1

CD163L1	32,39	0,0003	0,018	TC1200012748.hg.1
CD3E	32,33	0,0365	0,3204	TC1100009200.hg.1
CREB5	30,44	2,69E-08	8,24E-05	TC0700007034.hg.1
S1PR1	30,34	0,0004	0,0225	TC0100009241.hg.1
WLS	28,95	4,74E-05	0,0059	TC0100014531.hg.1
FCGR3A	27,66	3,62E-08	8,63E-05	TC0100016185.hg.1
CD96	27,26	0,163	0,6348	TC0300008320.hg.1
CIDEB	26,71	0,0006	0,0291	TC1400008752.hg.1
GPR84	26,68	2,28E-05	0,0039	TC1200010837.hg.1
VSIG4	25,97	4,51E-05	0,0059	TC0X00009911.hg.1
FOLR2	24,24	0,0002	0,0149	TC1100008341.hg.1
SAMSN1	23,64	0,0001	0,0121	TC2100007599.hg.1
RGL1	23,01	0,0001	0,0099	TC0100010874.hg.1
PLTP	23	4,79E-07	0,0003	TC2000009250.hg.1
LRRC25	22,46	5,71E-05	0,0068	TC1900010013.hg.1
CLEC4A	22,19	8,26E-08	0,0001	TC1200012593.hg.1
FCGR3B	22,04	2,76E-07	0,0002	TC0100016189.hg.1
PLAU	21,35	3,91E-05	0,0054	TC1000008054.hg.1
TNFSF13	20,3	6,60E-06	0,0017	TC1700012186.hg.1
C1QA	20,26	1,68E-05	0,0033	TC0100007290.hg.1
P3H2	20,04	0,0002	0,016	TC0300013513.hg.1
LGALS12	19,43	0,0017	0,0599	TC1100007897.hg.1
HPSE	19,35	3,26E-07	0,0002	TC0400011203.hg.1
CD3D	19,3	0,1188	0,557	TC1100012478.hg.1
MPEG1	19,23	2,16E-05	0,0037	TC1100010962.hg.1
LGMN	18,81	0,0004	0,0237	TC1400010012.hg.1
CD209	18,59	2,59E-05	0,0042	TC1900009493.hg.1
IL1B	18,42	0,0045	0,1023	TC0200013916.hg.1
TNFRSF11A	17,77	0,0027	0,0748	TC1800007508.hg.1
C1QB	17,32	0,0005	0,0267	TC0100007292.hg.1
IFITM3	16,84	0,0002	0,0163	TC1100009657.hg.1
FCGR1A	16,41	5,20E-05	0,0063	TC0100009866.hg.1
LY75-CD302; CD302; LY75	16,36	3,04E-06	0,001	TC0200014728.hg.1
LILRB5	15,81	1,65E-05	0,0032	TC1900011406.hg.1
ENPP2	14,62	0,0038	0,0911	TC0800011620.hg.1
FCGBP	14,43	0,0168	0,2126	TC1900010676.hg.1
LACC1	14,3	1,59E-05	0,0032	TC1300009956.hg.1
LGALS2	14,25	0,36	0,8157	TC2200008661.hg.1
ADAP2	13,89	2,46E-06	0,0009	TC1700012226.hg.1
MMP12	13,05	0,1788	0,6554	TC1100012134.hg.1
MAF	13,01	4,37E-06	0,0013	TC1600010951.hg.1
RUNX1	12,77	8,17E-05	0,0086	TC2100008562.hg.1
AP1S2	12,5	6,32E-06	0,0017	TC0X00009139.hg.1

HLA-DQA2	12,12	0,0003	0,017	TC0600007664.hg.1
F13A1	11,89	0,0011	0,046	TC0600010709.hg.1
ANLN	11,82	0,0456	0,3594	TC0700007198.hg.1
STEAP1	11,52	0,0015	0,0545	TC0700008292.hg.1
CD74	11,21	0,0094	0,1509	TC0500012470.hg.1
IPCEF1	11,1	0,0001	0,0112	TC0600014360.hg.1
PRC1	11,09	0,0172	0,2157	TC1500010463.hg.1
AP2A2	10,62	4,61E-07	0,0003	TC1100006500.hg.1
HLA-DQA1	10,42	0,0172	0,2157	TC0600007657.hg.1
NLRP3	10,42	1,08E-05	0,0024	TC0100012315.hg.1
TNFRSF11A	10,37	2,86E-05	0,0045	TC1800007506.hg.1
CSF2RA	10,21	0,0002	0,0138	TC0Y00006444.hg.1
GPR183	10,16	0,002	0,065	TC1300009598.hg.1
DOK2	10,03	6,30E-07	0,0004	TC0800009819.hg.1

[1]Two-sided p-values derived from one-way ANOVAs. [2]False discovery rate adjusted p-values. Macrophages were derived from 3 subjects (3 samples; n = 9) and induced microglia-like cells from 3 subjects (3 samples; n = 9). Only genes upregulated with a fold change > 20 are included in the table.

Supplementary Table 5. Affymetrix gene array characterization of iPSC-derived neural cultures.

Gene Symbol	Description	Fold Change	P-value[1]	FDR P-value[2]	Affymetrix Probe ID
ZIC1	*forebrain cortical*	1097,99	6,97E-06	0,0002	TC0300013886.hg.1
NCAM1	*pan-neuronal*	318,73	3,17E-07	3,11E-05	TC1100009068.hg.1
GRIA2	*AMPA receptors*	233,91	4,05E-08	9,54E-06	TC0400009110.hg.1
NR2F1	*cerebral cortex*	175,42	4,21E-05	0,0008	TC0500008086.hg.1
MAP2	*pan-neuronal*	161,43	1,14E-09	3,80E-06	TC0200010636.hg.1
DCX	*pan-neuronal*	155,87	5,86E-08	1,16E-05	TC0X00010516.hg.1
CXCR4	*neural progenitor*	92,32	3,11E-05	0,0006	TC0200014414.hg.1
MAPT	*pan-neuronal*	53,47	6,27E-07	4,83E-05	TC1700008082.hg.1
NCAM1	*pan-neuronal*	30,72	1,19E-05	0,0003	TC1100009075.hg.1
GRIN2B	*NMDA receptors*	29,31	1,24E-05	0,0003	TC1200009997.hg.1
RELN	*Telencephalic*	27,34	0,0014	0,0094	TC0700012126.hg.1
ANK2	*cerebral cortex / cerebellum*	14,54	2,23E-06	0,0001	TC0400008450.hg.1
GRIA1	*AMPA receptors*	14,07	1,15E-05	0,0003	TC0500009141.hg.1
CD44	*neural progenitor*	13,49	0,0067	0,0303	TC1100007273.hg.1
PAX6	*neural progenitor*	9,66	0,0042	0,0214	TC1100010456.hg.1
ASCL1	*Diencephalon*	7,91	8,80E-05	0,0013	TC1200008650.hg.1
S100B	*Astrocyte*	7,88	0,0002	0,0019	TC2100008477.hg.1
CACNA1C	*calcium channel*	6,71	0,0002	0,002	TC1200012570.hg.1
DLG4	*post-synaptic*	6,54	3,82E-05	0,0007	TC1700009619.hg.1
SNAP25	*pre-synaptic*	5,98	0,0001	0,0016	TC2000006688.hg.1
ZFPM2	*cerebral cortex*	5,1	0,0039	0,0201	TC0800012344.hg.1
SYP	*pre-synaptic*	4,19	0,0005	0,0046	TC0X00009661.hg.1
B3GAT2	*neural crest*	4,17	0,0002	0,0024	TC0600012257.hg.1
GPHN	*post-synaptic*	4,09	0,0002	0,002	TC1400007478.hg.1
FOXP2	*Diencephalon*	4,01	0,0465	0,1277	TC0700008849.hg.1
PROX1	*hippocampal / cerebellum*	3,74	0,0009	0,0067	TC0100011566.hg.1
NEUROD1	*Telencephalic*	3,47	0,0013	0,0088	TC0200016755.hg.1

SOX5	*Telencephalic*	3,03	0,0002	0,0026	TC1200010130.hg.1
GRIA3	*AMPA receptors*	2,93	0,0205	0,0697	TC0X00008316.hg.1
GRIA1	*AMPA receptors*	2,88	0,0025	0,0143	TC0500009147.hg.1
BSN	*pre-synaptic*	2,77	0,0037	0,0193	TC0300007385.hg.1
STX1A	*pre-synaptic*	2,66	0,0028	0,0159	TC0700011500.hg.1
GAD2	*cortical GABAergic neuron*	2,62	0,0163	0,0589	TC1000007068.hg.1
ZFPM2	*cerebral cortex*	2,55	0,0433	0,1213	TC0800012343.hg.1
TUBB3	*pan-neuronal*	2,51	0,0027	0,0155	TC1600011453.hg.1
SYN1	*pre-synaptic*	2,5	0,0004	0,0039	TC0X00009576.hg.1
SOX1	*telencephalic progenitor*	2,39	0,0087	0,0367	TC1300008059.hg.1
POU3F2	*Telencephalic*	2,12	0,0023	0,0135	TC0600008897.hg.1
CAMK2A	*post-synaptic*	2,06	0,0038	0,0197	TC0500012463.hg.1
FLT1	*Mesodermal*	-13,99	8,75E-07	5,94E-05	TC1300008463.hg.1
FOXO1	*hindbrain / cerebellum*	-14,66	8,97E-07	6,03E-05	TC1300008688.hg.1
DIAPH3	*cerebral cortex*	-17,43	6,25E-05	0,001	TC1300009088.hg.1
PROM1	*stem cell marker*	-25,74	8,28E-07	5,75E-05	TC0400012903.hg.1
ZFP42	*pluripotency marker*	-40,89	3,92E-08	9,54E-06	TC0400009588.hg.1
NANOG	*pluripotency marker*	-54,92	3,80E-08	9,50E-06	TC1200006688.hg.1
MKI67	*proliferation marker*	-65,39	2,51E-06	0,0001	TC1000012235.hg.1
POU5F1	*pluripotency marker*	-102,02	7,29E-09	4,90E-06	TC0600011406.hg.1
OTX2	*progenitor marker*	-102,16	2,57E-08	8,43E-06	TC1400009282.hg.1
LIN28A	*pluripotency marker*	-147,81	3,43E-09	4,72E-06	TC0100007457.hg.1

[1]Two-sided p-values derived from one-way ANOVAs. [2]False discovery rate adjusted p-values. iPSCs generated from n=2 subjects and iPSC-derived neurons generated from n=4 subjects. Genes were selected based on Zhang, Y., *et al.* (Rapid single-step induction of functional neurons from human pluripotent stem cells. *Neuron* **78**, 785-798 (2013)). In table only genes displaying a fold change > 2 (with P(FDR) < 0.05) are shown.

Supplementary Table 6. Clinical characteristics for participants in main experiments.

Experiment		SZ-SZ vs. HC-HC (pHrodo)	SZ-SZ vs. HC-HC (PSD-95)	SZ-SZ vs. HC-HC (co-culture)	SZ-SZ vs. SZ-HC vs. HC-HC (pHrodo)	SZ-SZ vs. HC-SZ vs. HC-HC (pHrodo)	SZ-SZ vs. SZ-HC vs. HC-HC (PSD-95)	SZ-SZ vs. HC-SZ vs. HC-HC (PSD-95)	Minocycline pre-treatment
SZ IMGs	PANSS	68 (19)	69 (18)	65 (9)	69 (26)	71 (28)	69 (32)	69 (31)	Not done
	IQ	85 (20)	94 (19)	67 (10)	82 (13)	82 (21)	82 (15)	82 (20)	Not done
	Vocab	39 (15)	50 (22)	39 (3)	38 (9)	37 (18)	38 (10)	47 (14)	Not done
	MR	43 (11)	43 (10)	36 (13)	43 (12)	43 (8)	43 (10)	42 (16)	Not done
	n	13	13	3	8	10	6	6	2
HC IMGs	IQ	109 (29)	111 (28)	90	104 (39)	117 (7)	99 (42)	117 (19)	116 (33)
	Vocab	52 (12)	53 (13)	44	52 (15)	54 (15)	51 (18)	58 (21)	55 (13)
	MR	48 (27)	53 (27)	45	51 (29)	62 (17)	47 (33)	58 (24)	61 (23)
	n	9	18	2	13	5	6	6	10
SZ SYN (or neural culture)	PANSS[5]	62 (18)	67 (23)	65 (25)	62	62 (18)	62	n/a	62
	IQ	89 (19)	95 (29)	101 (27)	86	89 (12)	86	n/a	101
	Vocab	43 (12)	46 (25)	49 (17)	40	43 (13)	40	n/a	49
	MR	44 (10)	47 (9)	46 (21)	43	43 (2)	43	n/a	52
	n	3	4	3	2	3	2	n/a	1
HC SYN (or neural culture)	IQ[4]	100 (36)	100 (27)	107	108 (15)	100 (36)	n/a	100 (36)	100 (36)
	Vocab[3]	52 (20)	52 (15)	51	56 (6)	52 (20)	n/a	52 (20)	52 (20)
	MR[2]	48[6] (22)	48 (17)	48	52 (12)	48 (22)	n/a	48 (22)	48 (22)
	n[1]	3	4	2	3	3	n/a	3	3

[1]Number of subjects. [2]Matrix Reasoning subtest – WASI-II. T-scores. [3] Vocabulary subtest – WASI-II. T-scores. [4]IQ composite score – WASI-II. T-scores. [5]Positive and Negative Syndrome Scale. Total score. [6]All data given as median with interquartile rang

All schizophrenia (SZ) subjects were males between 25 and 60 years old and healthy controls (HCs) were matched on sex and age. Mean age in SZ subjects was 40.3 years (SD: 10.2) and among HCs 42.6 years (12.6).

Supplementary Table 7. Details of antibodies used for immunohistochemistry (ICC).

Antibody	Company	Catalog number	Host species	Concentration
TMEM 119	Abcam	Ab185337	Rabbit	1:50
P2RY12	Alomone labs	Apr-020	Rabbit	1:100
PU.1	Abcam	Ab88082	Mouse	1:50
OCT 4	Cell signaling	2840	Rabbit	1:400
TRA 1-60	Abcam	Ab16288	Mouse	1:500
NESTIN	Emd millipore	Abd69	Rabbit	1:500
PAX6	Developmental studies hybridoma bank	Pax6	Mouse	1:100
SOX 1	Cell signaling	4194s	Rabbit	1:200
SOX 2	Cell signaling	3579s	Rabbit	1:200
MAP2	Abcam	Ab92434	Chicken	1:1000
BETA III TUBULIN	Millipore	Mab5564	Mouse	1:1000
PSD95	Abcam	Ab13552	Mouse	1:250
C4	Abcam	Ab173577	Rabbit	1:250
CD68	Abcam	Ab213363	Rabbit	1:100

See also Life Sciences Reporting Summary for details regarding validation.